



The four-point correlation function of the energy-momentum tensor in the free conformal field theory of a scalar field

Mirko Serino^a

Department of Physics, Ben Gurion University of the Negev, Beer Sheva 8410501, Israel

Received: 22 May 2020 / Accepted: 6 July 2020 / Published online: 30 July 2020
© The Author(s) 2020

Abstract We present an explicit momentum space computation of the four-point function of the energy-momentum tensor in 4 spacetime dimensions for the free and conformally invariant theory of a scalar field. The result is obtained by explicit evaluation of the Feynman diagrams by tensor reduction. We work by embedding the scalar field theory in a gravitational background consistently with conformal invariance in order to derive all the terms the correlator consists of and all the Ward identities implied by the requirements of general covariance and anomalous Weyl symmetry. We test all these identities numerically in several kinematic configurations. *Mathematica* notebooks detailing the step-by-step computation are made publicly available through a GitHub repository (<https://github.com/mirkos86/4-EMT-correlation-function-in-a-4d-CFT>). To the best of our knowledge, this is the first explicit result for the four-point correlation function of the energy-momentum tensor in a conformal and non supersymmetric field theory which is readily numerically evaluable in any kinematic configuration.

Contents

1 Introduction	1
2 Setting up the computation	3
2.1 The structure of the correlators: topologies and diagrams	4
2.2 Organization of the <i>Mathematica</i> files	7
3 Derivation of the transverse and trace Ward identities	7
4 Counterterms, anomalies and a preliminary test of the $4T$ correlator	9
5 Into the full calculation	12

5.1 The calculation of the four-point correlator	12
5.2 Analytical checks of the Ward identities for the $2T$ and $3T$	13
5.3 Numerical checks of the Ward identities for the $4T$ correlator	14
5.4 Discussion about numerical stability	15
6 Conclusions and perspectives	17
A Conventions	18
A.1 Conventions for signs and momentum space correlators definition	18
A.2 Weyl invariant and Euler density in 4d	18
A.3 Vanishing of the Euler counterterms	19
B Functional derivatives	19
B.1 Basic functional derivatives	19
B.2 Interaction vertices of the scalar field with gravitons	20
References	21

1 Introduction

The energy-momentum tensor is the most universal operator for conformal field theories (CFTs). Therefore, its correlation functions are natural objects to study in any CFT.

It has been known for a long time that conformal invariance completely fixes the two-point correlation function of the energy-momentum tensor, whereas the three-point function in 4d is fixed up to three scalar coefficients, which can be inferred by computing the correlator for the field theories of a scalar, a fermion and an abelian gauge field. This was first dealt with in coordinate space for three-point correlators of operators up to spin 2 in [1, 2], by solving all the constraints implied by the full conformal group. An analogous program in momentum space, based on the solution of all the conformal group Ward identities to constrain the 3 point functions of scalars, vector currents and energy-momentum tensors modulo a few constants was carried out much more recently [3–5] and found to be perfectly consistent with the other approach,

In loving memory of Giuseppe Serino
* April 1st 1956 † December 4th 2018.

^ae-mail: mirkos.serino@gmail.com (corresponding author)

although mathematically very different. A different approach in momentum space to the three-point function of the energy-momentum tensor has been pursued in [6], where an explicit diagrammatic computation was performed (and published in a partially on-shell kinematics). The consistency of the two momentum space approaches was later verified by [7].

Much more involved is the case for four-point functions, because the conformal group does not uniquely constrain them. For the case of scalars, Polyakov first showed that the four-point correlator is fixed up to a function of the coordinates cross ratios [8],

$$\begin{aligned} \langle \mathcal{O}(x_1) \mathcal{O}(x_2) \mathcal{O}(x_3) \mathcal{O}(x_4) \rangle &= \frac{f_1(u, v)}{(x_1 - x_2)^{2\Delta} (x_3 - x_4)^{2\Delta}}, \\ u &= \frac{(x_1 - x_2)^2 (x_3 - x_4)^2}{(x_1 - x_3)^2 (x_2 - x_4)^2}, \\ v &= \frac{(x_1 - x_4)^2 (x_2 - x_3)^2}{(x_1 - x_3)^2 (x_2 - x_4)^2}. \end{aligned} \quad (1)$$

As for operators with spin, though much is already known in position space [9], very little is known about four-point correlation functions in momentum space and the connection between the two is not trivial, as discussed thoroughly in [6]. One very powerful and popular approach to CFT dynamics is the so called conformal bootstrap [10–12], which allows to constrain four-point functions through consistency constraints connecting different conformal blocks representations of the same four-point function. So far, it has been successfully applied mainly to the case of scalar operators. One exception is a very recently proposed approach to conformal blocks for any spin [13, 14], which was applied to two, three and four-point functions [15–17], though not to the four-point function of the energy-momentum tensor due to its sheer complexity.

The number of unrestricted degrees of freedom for the four-point function of the energy-momentum tensor in general dimensions was already determined in [18], where the number of effectively independent constraints provided by the Ward identities stemming from the requirements of both special conformal invariance and energy-momentum conservation was nailed down. There have been works – all of them in the context of the AdS/CFT correspondence – which have investigated the four-point function of the energy-momentum tensor. The first one has explored the structure of some contributions to the four-point function through an OPE analysis [19]. Later, the most general structure in coordinate space of the correlator was pinned down in [20, 21]. By different means, analogous structures were conjectured in [22] and later proven to be correct in [23].¹ So far, however, no explicit result has been presented in momentum space, except for the

case of superconformal $\mathcal{N} = 4$ [24], let alone any which lends itself to numerical evaluation.

With these recent advances in mind, in the present paper we present an explicit perturbative computation of the four-point function of the energy-momentum tensor in the simplest possible conformal field theory in 4d which admits a Lagrangian realization and thus a perturbative approach: a free scalar field. It is paramount to notice that the fact that the theory is free does not just make calculations simpler; it is such that the 1 loop results for the four-point function (or lower and higher point functions as well), which can be computed using perturbation theory, are also exact, because no higher order loops are admitted. In this way, the perturbative calculation produces a result equivalent to what would be produced by non perturbative methods, though unfortunately way less compact because of redundancies.

We provide our results in a set of ancillary *Mathematica* files stored in the public GitHub repository quoted in the abstract. In these files, the reader is guided step by step through the computation of the two, three and four-point correlators of the energy-momentum tensor for the theory at hand, as well as through the tests of the Ward identities stemming from the requirements of energy-momentum conservation and anomalous Weyl symmetry. The *Mathematica* notebooks code features plenty of comments which make them readily usable and (hopefully) understandable. We exploit the recently developed *Package-X* [25, 26] together with its *CollierLink* extension for fast numerical evaluation of tensor integrals through the *COLLIER* library [27–30].

We did not attempt to track down the few [18] independent tensor structures our correlator should ultimately consist of, by itself a very demanding task given the sheer dimensions of the four-point function. We leave an attempt in this direction for possible future work.

The main reason why we undertook this calculation, beside the fact that we could do it, is the hope that our result could serve as a benchmark check (most probably numerical, though the result itself is fully analytical) for computations carried out with non perturbative methods, e.g. the conformal bootstrap for fields with spin.

This paper is organized as follows. In Sect. 2 we describe the setup of our calculation and the diagrammatic expansion of all the energy-momentum tensor correlators through four point, in order to make our discussion as self-contained as possible, beside providing a detailed explanation of the structure of the *Mathematica* files. In Sect. 3 we derive all the Ward identities stemming from the requirements of general covariance (named transverse Ward identities hereafter) and Weyl invariance (named trace Ward identities hereafter), the latter of which feature a well known trace anomaly. In Sect. 4 we describe the computation of the 1 loop counterterms and the anomaly functional for the energy-momentum tensor correlators through four point and how we can check them against

¹ We are grateful to Evgeny Skvortsov and Johanna Erdmenger for pointing out these references.

each other independently of the Feynman diagram computations; the counterterms are then used for a preliminary check of the diagrammatic expansion, by comparing them to the UV pole of the correlators. In Sect. 5 we illustrate in detail the *Mathematica* implementation of our calculation and the procedure followed to analytically test the Ward identities for the two and three-point correlators and to test them numerically for the four-point correlator. Indeed, the last task is too massive to be dealt with analytically. In this section we also give plenty of detail on the implementation of all our computations in *Mathematica* through *Package-X* and *CollierLink*. Section 6 presents our conclusions and perspectives for further work.

2 Setting up the computation

This introductory section closely follows Chapter 2 of [31]. For details about the general relation between conformal invariance in flat space and Weyl invariance in curved space see [32]; here we assume that Weyl invariance in curved space is interchangeable with conformal invariance in flat space, as it is actually the case for the theory we are dealing with.

The standard definition of the energy-momentum tensor (EMT in the following) in a classical field theory described by an action \mathcal{S} is given in terms of a functional derivative w.r.t. the metric tensor $g_{\mu\nu}(z)$ once the theory has been embedded in curved space, i.e.

$$\begin{aligned} T^{\mu\nu}(z) &= -\frac{2}{\sqrt{g_z}} \frac{\delta \mathcal{S}}{\delta g_{\mu\nu}(z)} \\ &= g^{\mu\alpha}(z) g^{\nu\beta}(z) \frac{2}{\sqrt{g_z}} \frac{\delta \mathcal{S}}{\delta g^{\alpha\beta}(z)}, \end{aligned} \tag{2}$$

where $\det g_{\mu\nu}(z) \equiv g_z$.

We introduce the generating functional of the theory in Euclidean conventions, which we call \mathcal{W} ,

$$\mathcal{W} = \frac{1}{\mathcal{N}} \int \mathcal{D}\Phi e^{-\mathcal{S}}, \tag{3}$$

where \mathcal{N} is a normalization constant and Φ generally indicates the quantum fields of the theory. Given (2), the vacuum expectation value (vev) of the EMT is

$$\langle T^{\mu\nu}(z) \rangle_s = \frac{2}{\sqrt{g_z}} \frac{\delta \mathcal{W}}{\delta g_{\mu\nu}(z)}, \tag{4}$$

with the subscript s (which stands for ‘‘source’’) meaning that the background fields are not switched off. Dependence on coordinates will be occasionally dropped if it is not strictly necessary to the understanding of formulas.

In a conformal field theory the trace of the EMT vanishes at the classical level upon using the equations of motion, $T^\mu{}_\mu = 0$. As for the vev of the EMT, this relation is modified by the well known trace anomaly [33,34]

$$\begin{aligned} g_{\mu\nu} \langle T^{\mu\nu} \rangle_s &\equiv \mathcal{A}[g] \\ &= \sum_{I=f,s,v} n_I \left[\beta_a(I) F + \beta_b(I) G + \beta_c(I) \square R + \beta_d(I) R^2 \right], \end{aligned} \tag{5}$$

where g is a short-hand notation for the background metric. The coefficients κ , β_a , β_b , β_c and β_d depend on the field content of the Lagrangian theory and we have a multiplicity factor n_I for each particle species. Eq. (5) is a reorganization in terms of the squared Weyl tensor and the Euler characteristic of 4d spacetime (see Appendix A.2) of the most general linear combination of the squares of the Riemann tensor and its contractions. The coefficient of R^2 must actually vanish identically

$$\beta_d \equiv 0, \tag{6}$$

since it does not satisfy the Wess-Zumino consistency condition for conformal anomalies [35,36]. In addition, the value of β_c is regularization dependent, corresponding to the fact that it can be changed by the addition of an arbitrary local term in the effective action proportional to the integral of R^2 [33]. In particular, the values for the anomaly coefficients which we will use here for one single scalar field, i.e.

$$\beta_a = \frac{3}{5760 \pi^2}, \quad \beta_b = -\frac{1}{5760 \pi^2} \tag{7}$$

for which one finds the constraint [33,34]

$$\beta_c = -\frac{2}{3} \beta_a. \tag{8}$$

The trace anomaly functional only depends on the metric tensor, $\mathcal{A} \equiv \mathcal{A}[g]$,

$$g_{\mu\nu} \langle T^{\mu\nu} \rangle_s = \beta_a \left(F - \frac{2}{3} \square R \right) + \beta_b G \tag{9}$$

The conformally invariant action for a scalar field coupled to gravity in 4 dimensions is given by

$$\mathcal{S} = \frac{1}{2} \int d^4x \sqrt{g} \left[g^{\mu\nu} \nabla_\mu \phi \nabla_\nu \phi - \chi R \phi^2 \right]. \tag{10}$$

Here χ is the parameter corresponding to the term of improvement obtained by coupling ϕ^2 to the scalar curvature R . In general dimensions d , $\chi = 1/4 (d - 2)/(d - 1)$ gives a CFT, so that $\chi = 1/6$ gives a classically conformal invariant theory in $d = 4$, whose EMT is

$$\begin{aligned} T_S^{\mu\nu} &= \nabla^\mu \phi \nabla^\nu \phi - \frac{1}{2} g^{\mu\nu} g^{\alpha\beta} \nabla_\alpha \phi \nabla_\beta \phi \\ &\quad + \chi \left[g^{\mu\nu} \square - \nabla^\mu \nabla^\nu + \frac{1}{2} g^{\mu\nu} R - R^{\mu\nu} \right] \phi^2. \end{aligned} \tag{11}$$

The explicit expressions for the vertices involving one or more metric tensors, which can be computed by functional differentiating the action, have been already given in [37] and are also here collected in Appendix B for completeness,

beside being explicitly computed in the attached *Mathematica* file *functional_derivatives.nb*. For further details about our conventions on covariant derivatives, Christoffel symbols and the Riemann tensor, see Appendix A.

One remark is appropriate at this point: if we employed the d -dimensional value of the improvement parameter $\chi = (d - 2)/[4(d - 1)] = 6 - \epsilon/18$, there should be some extra finite terms in the correlators we compute than when employing directly $\chi = 1/6$, because of the interplay between $\epsilon/18$ and the UV pole $\propto 1/\epsilon$, at least in principle. If these terms survived in the $d \rightarrow 4$ limit, then this result would differ from the computation performed directly with $\chi = 1/6$. This actually happens for individual diagrams. Now, if the limit of a d -dimensional correlators were not the 4d correlators, it would mean that conformal correlators depend on the regularization technique employed to compute them in perturbation theory, for this is manifestly an issue specific to Dimensional Regularization (DR hereafter). This is patently inconsistent and suggests that a further consistency condition - beside all the Ward identities we explicitly check - is that these extra terms must cancel out when all the pieces making up conformal correlators are put together. This turns out to be the case and the explicit check is left to the interested reader.

2.1 The structure of the correlators: topologies and diagrams

Our first step is to exploit the background field method to build the correlation function of n energy-momentum tensors and evaluate it diagrammatically at 1 loop. Since the theory is non interacting, as the scalar field is not coupled to any other quantum field, there are no higher order perturbative contributions, as one can easily verify. We work in DR.

Our definition of the n -EMT correlators (also nT below) is that of a symmetric n th functional derivative of \mathcal{W} w.r.t. the metric tensor,

$$\begin{aligned} &\langle T^{\mu_1\nu_1}(x_1) \dots T^{\mu_n\nu_n}(x_n) \rangle \\ &= \left[\frac{2^n}{\sqrt{g_{x_1}} \dots \sqrt{g_{x_n}}} \frac{\delta^n \mathcal{W}}{\delta g_{\mu_n\nu_n}(x_n) \dots \delta g_{\mu_1\nu_1}(x_1)} \right] \Big|_{g_{\mu\nu}=\delta_{\mu\nu}} \\ &= 2^n \frac{\delta^n \mathcal{W}}{\delta g_{\mu_n\nu_n}(x_n) \dots \delta g_{\mu_1\nu_1}(x_1)} \Big|_{g_{\mu\nu}=\delta_{\mu\nu}}. \end{aligned} \tag{12}$$

Symmetry comes from leaving factors $2/\sqrt{g}$ outside of the derivatives. Given that field theory in Minkowski space is simply given by an analytic continuation from 4d Euclidean theory we work with through $\delta_{\mu\nu} \rightarrow \eta_{\mu\nu}$, we will also refer to this vertex as to the “ n -graviton” vertex. We choose to denote such correlators, which contain contact terms, with small angular brackets ($\langle \rangle$).

Contact terms are characterized in coordinate space by the presence of at least two gravitons at the same spacetime point. Such contact terms are absent by definition in the expression

of correlation functions given by the expectation value of the product of n EMT’s, which are denoted with large angular brackets ($\langle \rangle$) as in

$$\begin{aligned} &\langle T^{\mu_1\nu_1}(x_1) \dots T^{\mu_n\nu_n}(x_n) \rangle \\ &= \frac{1}{\mathcal{N}} \int \mathcal{D}\Phi T^{\mu_1\nu_1}(x_1) \dots T^{\mu_n\nu_n}(x_n) e^{-S} \Big|_{g_{\mu\nu}=\delta_{\mu\nu}}. \end{aligned} \tag{13}$$

This distinction will not only apply to the vev of n insertions of the EMT, but also to contact terms and, in general, to all the correlation functions appearing in this paper.

It will also be useful to introduce the following notation to represent the functional derivative with respect to the background metric evaluated in flat space,

$$\begin{aligned} &[f(x)]^{\mu_1\nu_1\mu_2\nu_2\dots\mu_n\nu_n}(x_1, x_2, \dots, x_n) \\ &\equiv \frac{\delta^n f(x)}{\delta g_{\mu_n\nu_n}(x_n) \dots \delta g_{\mu_2\nu_2}(x_2) \delta g_{\mu_1\nu_1}(x_1)} \Big|_{g_{\mu\nu}=\delta_{\mu\nu}}. \end{aligned} \tag{14}$$

Since with our conventions all the functional derivatives will be taken w.r.t. the metric tensor with lower indices, which thus produces upper indices, possible functional derivatives with lower indices will mean just

$$\begin{aligned} &[f(x)]_{\mu_1\nu_1\dots\mu_n\nu_n}(x_1, x_2, \dots, x_n) \\ &\equiv \delta_{\mu_1\alpha_1} \delta_{\nu_1\beta_1} \dots \delta_{\mu_n\alpha_n} \delta_{\nu_n\beta_n} \\ &[f(x)]^{\alpha_1\beta_1\alpha_2\beta_2\dots\alpha_n\beta_n}(x_1, x_2, \dots, x_n). \end{aligned} \tag{15}$$

In order to make tensorial expressions more compact, if we happen to contract two indices with the metric, we will stack the two contracted indices on top of each other, as in

$$\begin{aligned} &[\mathcal{S}]_{\mu_1}^{\mu_1} \equiv [\mathcal{S}]^{\mu_1\nu_1} \delta_{\mu_1\nu_1} \quad \text{or} \\ &[\mathcal{S}]_{\mu_1\mu_2}^{\mu_1\mu_2} \equiv [\mathcal{S}]^{\mu_1\nu_1\mu_2\nu_2} \delta_{\mu_1\nu_1} \delta_{\mu_2\nu_2}. \end{aligned} \tag{16}$$

With these definitions, a single functional derivative of the action in a correlation function is always equivalent, modulo a factor, to an insertion of a $T^{\mu\nu}$ in the flat limit, since

$$\begin{aligned} &[\mathcal{S}]^{\mu_1\nu_1}(x_1) \equiv \frac{\delta \mathcal{S}}{\delta g_{\mu_1\nu_1}(x_1)} \Big|_{g_{\mu\nu}=\delta_{\mu\nu}} \\ &= -\frac{1}{2} T^{\mu_1\nu_1}(x_1). \end{aligned} \tag{17}$$

To begin with the easiest correlation functions, the definition of Eq. (12) implies that the two-point function is

$$\begin{aligned} &\langle T^{\mu_1\nu_1}(x_1) T^{\mu_2\nu_2}(x_2) \rangle \\ &= 4 \left[\langle [\mathcal{S}]^{\mu_1\nu_1}(x_1) [\mathcal{S}]^{\mu_2\nu_2}(x_2) \rangle - \langle [\mathcal{S}]^{\mu_1\nu_1\mu_2\nu_2}(x_1, x_2) \rangle \right]. \end{aligned} \tag{18}$$

The last term on the right hand side of the equation above, which is a massless tadpole, can be set to zero in DR, so that the $2T$ correlation function, obtained by differentiation of the

generating functional, coincides with the quantum average of two energy-momentum tensors

$$\begin{aligned} &< T^{\mu_1\nu_1}(x_1)T^{\mu_2\nu_2}(x_2) > \\ &= 4\langle [S]^{\mu_1\nu_1}(x_1)[S]^{\mu_2\nu_2}(x_2) \rangle = \langle T^{\mu_1\nu_1}(x_1)T^{\mu_2\nu_2}(x_2) \rangle. \end{aligned} \tag{19}$$

This will not be true for higher order correlation functions, where non vanishing contact terms also appear. For the sake of completeness, the 1 loop contribution to the two-point correlation function is illustrated in Fig. 2.

The 3T correlator functional expansion is given instead by

$$\begin{aligned} &< T^{\mu_1\nu_1}(x_1)T^{\mu_2\nu_2}(x_2)T^{\mu_3\nu_3}(x_3) > \\ &= \langle T^{\mu_1\nu_1}(x_1)T^{\mu_2\nu_2}(x_2)T^{\mu_3\nu_3}(x_3) \rangle \\ &\quad - 4 \left(\langle [S]^{\mu_1\nu_1\mu_2\nu_2}(x_1, x_2)T^{\mu_3\nu_3}(x_3) \rangle + 2 \text{ perm.} \right) \\ &\quad - 8 \langle [S]^{\mu_1\nu_1\mu_2\nu_2\mu_3\nu_3}(x_1, x_2, x_3) \rangle \end{aligned} \tag{20}$$

whose right hand side is expressed in terms of one ordinary three-point correlator plus extra contact terms. The additional terms obtained by permutation are such as to render symmetric the right hand side.

The first term on the right hand side of Eq. (20) is an ordinary three-point function, whose connected component is given, at 1 loop, by the triangle diagram of Fig. 3, while the last term is a massless tadpole (see Fig. 1)², which can be set to zero

$$\langle [S]^{\mu_1\nu_1\mu_2\nu_2\mu_3\nu_3}(x_1, x_2, x_3) \rangle = 0. \tag{21}$$

In the 3T case, contact terms have the topology of a bubble and are generated by correlators containing insertions of the second functional derivative of the action w.r.t. to the metric. Their general structure is shown in Fig. 3 and each one of them is simply obtained by assigning the momenta to the diagram according to one of the the three possible groupings.

Moving finally to the 4T case, a similar expansion holds and is given by

$$\begin{aligned} &< T^{\mu_1\nu_1}(x_1)T^{\mu_2\nu_2}(x_2)T^{\mu_3\nu_3}(x_3)T^{\mu_4\nu_4}(x_4) > \\ &= \langle T^{\mu_1\nu_1}(x_1)T^{\mu_2\nu_2}(x_2)T^{\mu_3\nu_3}(x_3)T^{\mu_4\nu_4}(x_4) \rangle \\ &\quad - 4 \left[\langle [S]^{\mu_1\nu_1\mu_2\nu_2}(x_1, x_2)T^{\mu_3\nu_3}(x_3)T^{\mu_4\nu_4}(x_4) \rangle + 5 \text{ perm.} \right] \\ &\quad + 16 \left[\langle [S]^{\mu_1\nu_1\mu_2\nu_2}(x_1, x_2)[S]^{\mu_3\nu_3\mu_4\nu_4}(x_3, x_4) \rangle + 2 \text{ perm.} \right] \\ &\quad - 8 \left[\langle [S]^{\mu_1\nu_1\mu_2\nu_2\mu_3\nu_3}(x_1, x_2, x_3)T^{\mu_4\nu_4}(x_4) \rangle + 3 \text{ perm.} \right] \\ &\quad - 16 \langle [S]^{\mu_1\nu_1\mu_2\nu_2\mu_3\nu_3\mu_4\nu_4}(x_1, x_2, x_3, x_4) \rangle \end{aligned} \tag{22}$$

with

$$\langle [S]^{\mu_1\nu_1\mu_2\nu_2\mu_3\nu_3\mu_4\nu_4}(x_1, x_2, x_3, x_4) \rangle = 0, \tag{23}$$

² All Feynman diagrams were drawn with *feynMF*. [38].

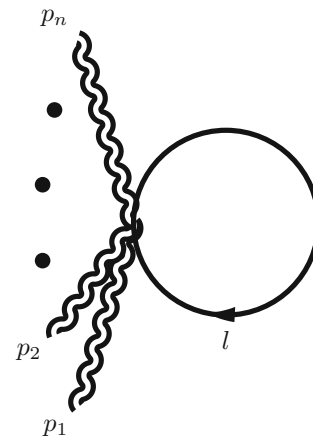


Fig. 1 The general topology of the vanishing 1-point contributions

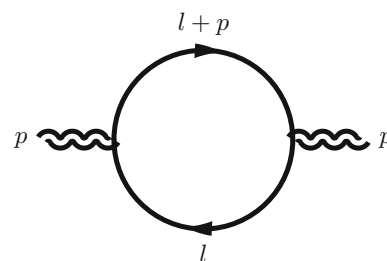


Fig. 2 The only 1 loop contribution to the two-point correlation function

being a massless tadpole contribution. In this case the perturbative expansion generates three diagrams of box type, represented by the Green function with 4 EMT insertions on the right hand side of (22), plus triangle, bubble and tadpole diagrams generated by the contact terms and graphically represented in Figs. 4 and 5.

The analysis of these contributions is more involved compared to the 3T case. In Figs. 4 and 5 we illustrate the general structures of the four kinds of diagrams involved. The momenta running through them in addition to the loop momentum *l* must be replaced by the specific assignments detailed below. Later, when we illustrate the implementation of the computation in *Mathematica*, we will refer to these basic diagrams corresponding to inequivalent topologies as *blueprint diagrams*.

For each topology we have a different number of contributions, corresponding to cyclically inequivalent orderings of the external momenta.

For the square topology, the 3 distinct contributions can be parametrized, for example, by the following three assignments of momenta (compare to the first diagram in Fig. 4)

$$\begin{aligned} (p_{i_1}, p_{i_2}, p_{i_3}, p_{i_4}) &= \begin{cases} (p_2, p_3, p_4, p_1) \\ (p_3, p_4, p_2, p_1) \\ (p_4, p_2, p_3, p_1) \end{cases} \\ q_1 &= p_{i_1}, \quad q_2 = p_{i_1} + p_{i_2}, \end{aligned}$$

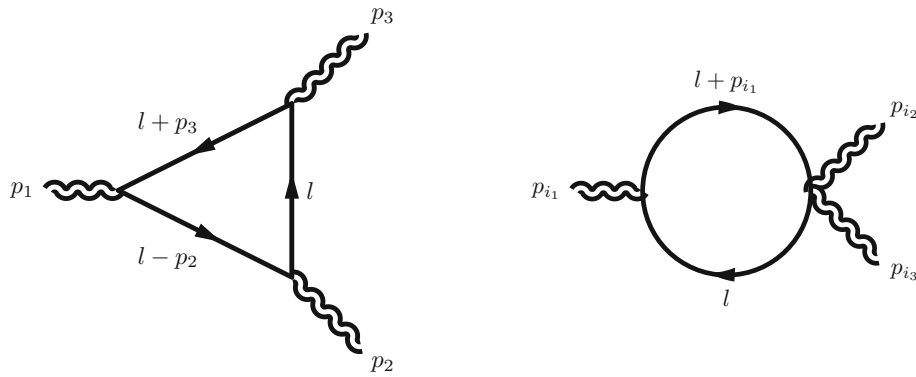


Fig. 3 The topologies contributing to the $\langle TTT \rangle$ correlation function. All the external momenta are incoming

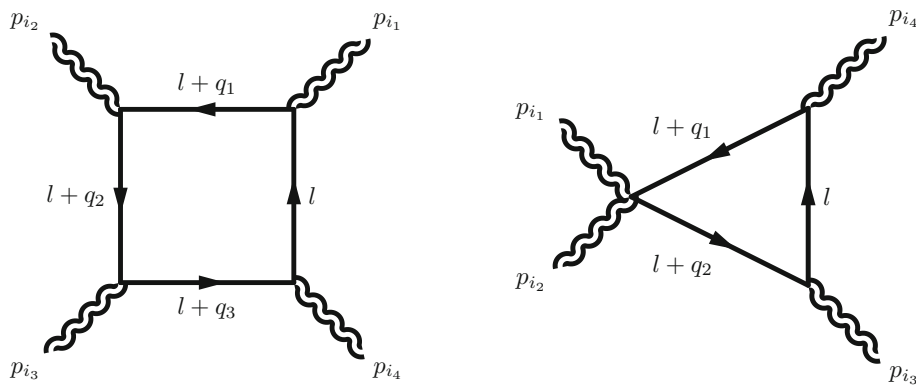


Fig. 4 The square and triangle topologies contributing to the $\langle TTTT \rangle$ correlation function. All the external momenta are incoming

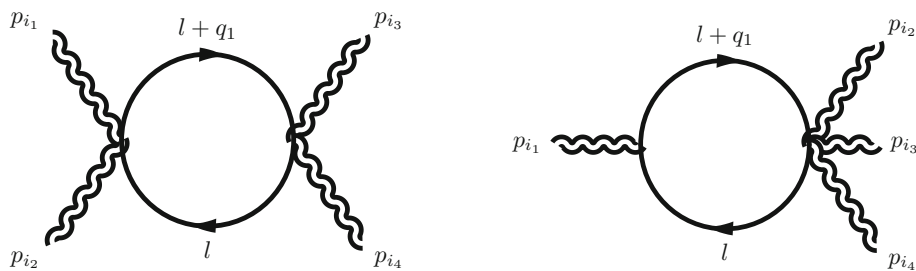


Fig. 5 The two kinds of bubble topology contributing to the $\langle TTTT \rangle$ correlation function in a scaleless theory. All the external momenta are incoming

$$q_3 = p_{i_1} + p_{i_2} + p_{i_3} = -p_{i_4} \tag{24}$$

For the triangle topology, there are the following 6 distinct contributions

$$(p_{i_1}, p_{i_2}, p_{i_3}, p_{i_4}) = \begin{cases} (p_1, p_2, p_3, p_4) \\ (p_1, p_3, p_2, p_4) \\ (p_1, p_4, p_2, p_3) \\ (p_2, p_3, p_1, p_4) \\ (p_2, p_4, p_1, p_3) \\ (p_3, p_4, p_1, p_2) \end{cases} \tag{25}$$

$$q_1 = p_{i_4}, \quad q_2 = -p_{i_3}.$$

As for the two bubble topologies, we choose to distinguish them through the nomenclature of 22-bubble and 31-bubble, the figures standing for the numbers of gravitons meeting in each of their respective vertices.

The 3 contributions for the 22-bubble are

$$(p_{i_1}, p_{i_2}, p_{i_3}, p_{i_4}) = \begin{cases} (p_1, p_2, p_3, p_4) \\ (p_1, p_3, p_2, p_4) \\ (p_1, p_4, p_2, p_3) \end{cases} \tag{26}$$

$$q_1 = p_{i_1} + p_{i_2}.$$

The 4 inequivalent contributions for the 31-bubbles are instead

$$(p_{i_1}, p_{i_2}, p_{i_3}, p_{i_4}) = \begin{cases} (p_1, p_2, p_3, p_4) \\ (p_2, p_1, p_3, p_4) \\ (p_3, p_1, p_2, p_4) \\ (p_4, p_1, p_2, p_3) \end{cases} \\ q_1 = p_{i_1}. \quad (27)$$

The task of computing the three-point function in a completely off-shell configuration and checking at the same time the transverse and trace Ward identities was already performed in [6], but only the result in a partially on-shell configuration was explicitly given. Now we face a more demanding task, which is the computation of the four-point function in a completely off-shell kinematics. This was made possible by the development of *Package-X* [26], a *Mathematica* package for tensor algebra and automatic reduction of 1 loop tensor integrals of any rank in arbitrary even dimensions. We detail the computation in Sect. 5. For now, we just mention that also the step-by-step computations of the two and (much more significantly) the three-point functions are made available, so as to give the reader a full overview of the automated procedure in simpler setups, beside the target case of the $4T$.

The building blocks of our computation are the scalar-graviton interaction vertices, which we report in Appendix B. Although we were completely confident about their calculation and we tested *Package-X* extensively by reproducing all of our previous results of [6] and a few other field theory results, the reduction of rank-8 tensor integrals still was an uncharted territory. Just as it was the case for the $3T$, we checked all of our computations by testing the transverse and trace Ward identities our four-point correlator was supposed to satisfy, which we derive in Sect. 3.

2.2 Organization of the *Mathematica* files

This is a quick overview of the files developed in order to perform and test our calculation of the 4-point function. The same picture is given by the README file stored in our repository. Some of the calculations can be quite time consuming and the numerical checks of the Ward identities for the four point function requires your computer to have at least 25 GB of memory at its disposal in order not to crush.

Some necessary requirements on the machine: *Mathematica* (version 10.1 or higher); the additional packages *Package-X* and *CollierLink* must be loaded on the machine where the notebooks are run. Beside, the notebook *functional_derivatives.nb* must be run once in order to be able to run the rest of the calculation, particularly *correlators_calculation.nb*, which must in turn be run in order to generate the correlation functions which are checked by *ward_identities.nb*.

Here follows a concise description of the scope and purpose of each notebook:

- The notebook *tensor_bases/tensor_bases_generation.nb* generates the 4 files *tensmom#rank##*. As the name suggests, the tensors in each of these files span a complete basis of tensors which are rank-## products of the metric tensor and # independent momenta. They are needed to check the Ward identities for the three and four-point correlation functions.
- *functional_derivatives.nb* generates the file *all_functional_derivatives*. As detailed in the paper, our computation requires heavy use of tensor structures: rank-2, 4 and 6 trace anomalies for the two, three and four-point functions, rank-4, 6 and 8 counterterms for the very same correlators. All of them are obtained by functionally differentiating scalars consisting of algebraic combinations of the Riemann tensor, the Ricci tensor and the Ricci scalar. The notebook starts by explaining the simplest functional derivatives of the metric tensor and goes on all the way up to anomalies, counterterms and interaction vertices of the scalar with the background gravitational field, introducing gradually more complex structures. The second part of the notebook checks that the counterterms and the anomalies, which are computed non perturbatively, obey all the constraints they are supposed to. This is needed to make us more confident about our explicit calculations of the Green functions, provided that their divergent parts match the counterterms (they do indeed) and that they pass the check of the trace Ward identities with the anomalies (they do as well).
- *correlators_calculation.nb* explicitly computes the two, three and four-point functions, checks that they match the counterterms computed in *functional_derivatives.nb* and stores them in 3 files: *T2_scalar*, *T3_scalar* and *T4_scalar*.
- The .jpg files in the “figures” folder are simply graphical representations of the diagrams computed in *correlators_calculation.nb* and of the vertices computed in *functional_derivatives.nb*, which are loaded in the same notebooks just above the line of code computing each of them.
- The notebook *ward_identities.nb* checks the Ward identities for all of our correlation functions; analytically for two and three-point, numerically for four-point.
- The notebook *vanishing_euler_ct.nb* proves that the Euler counterterm for the 4-point function actually vanishes in 4d (see Sect. 4).

3 Derivation of the transverse and trace Ward identities

In this section, we derive the Ward identities stemming from the requirements of invariance of the generating functional under general diffeomorphisms and Weyl transformations. We call them transverse and trace Ward identities respec-

tively. We proceed with a derivation of the relevant Ward identities satisfied by the two, three and four-point functions of the EMT.

Invariance under diffeomorphisms is defined by the condition of general covariance of the generating functional $\mathcal{W}[g]$, which translates into

$$\begin{aligned} \nabla_{v_1} \langle T^{\mu_1 v_1}(x_1) \rangle_g &= \nabla_{v_1} \left(\frac{2}{\sqrt{g_{x_1}}} \frac{\delta \mathcal{W}[g]}{\delta g_{\mu_1 v_1}(x_1)} \right) \\ &= \partial_{v_1} \langle T^{\mu_1 v_1}(x_1) \rangle_g \\ &\quad - \Gamma_{\kappa v_1}^{\mu_1} \langle T^{\kappa v_1}(x_1) \rangle_g - \Gamma_{v_1 \kappa}^{v_1} \langle T^{\mu_1 \kappa}(x_1) \rangle_g \\ &\Rightarrow 2 \partial_{v_1} \langle \frac{\delta \mathcal{W}}{\delta g_{\mu_1 v_1}(x)} \rangle_g - \Gamma_{\kappa v_1}^{\mu_1} \\ &\quad \langle \frac{\delta \mathcal{W}}{\delta g_{\kappa v_1}(x_1)} \rangle_g = 0, \end{aligned} \tag{28}$$

where in the last step, crucially for the symmetry of the correlators in the derived Ward identities below, we have exploited the cancellation of the last term on the rhs of the second line with the derivative of $1/\sqrt{g_{x_1}}$.

The Ward identities for symmetric correlators we are after are obtained by functional differentiation of Eq. (28) as many times as it takes to get the correlator we are interested in, followed by taking the flat limit.

For the $2T$ we have the well known transverse condition,

$$\partial_{v_1} \langle T^{\mu_1 v_1}(x_1) T^{\mu_2 v_2}(x_2) \rangle = 0. \tag{29}$$

For the $3T$ we see an already non trivial rhs showing up

$$\begin{aligned} \partial_{v_1} \langle T^{\mu_1 v_1}(x_1) T^{\mu_2 v_2}(x_2) T^{\mu_3 v_3}(x_3) \rangle \\ = -2 \left[\Gamma_{\kappa v_1}^{\mu_1}(x_1) \right]^{\mu_2 v_2}(x_2) \langle T^{\kappa v_1}(x_1) T^{\mu_3 v_3}(x_3) \rangle \\ - 2 \left[\Gamma_{\kappa v_1}^{\mu_1}(x_1) \right]^{\mu_3 v_3}(x_3) \langle T^{\kappa v_1}(x_1) T^{\mu_2 v_2}(x_2) \rangle. \end{aligned} \tag{30}$$

Much more involved is the case for the $4T$, whose transverse Ward identity in coordinate space is given by

$$\begin{aligned} \partial_{v_1} \langle T^{\mu_1 v_1}(x_1) T^{\mu_2 v_2}(x_2) T^{\mu_3 v_3}(x_3) T^{\mu_4 v_4}(x_4) \rangle \\ = -2 \left[\Gamma_{\kappa v_1}^{\mu_1}(x_1) \right]^{\mu_2 v_2}(x_2) \langle T^{\kappa v_1}(x_1) T^{\mu_3 v_3}(x_3) T^{\mu_4 v_4}(x_4) \rangle \\ + 2 \left[\Gamma_{\kappa v_1}^{\mu_1}(x_1) \right]^{\mu_3 v_3 \mu_4 v_4}(x_3, x_4) \langle T^{\kappa v_1}(x_1) T^{\mu_2 v_2}(x_2) \rangle \\ + (2 \leftrightarrow 3, 2 \leftrightarrow 4). \end{aligned} \tag{31}$$

The functional derivatives of the Christoffel symbol, obtained from the expansion of the covariant derivatives which appear in previous equations, are explicitly given in Appendix B.

Before moving to momentum space, we point out that the Fourier transform formula is defined by (54), where all the momenta are incoming. We keep this convention throughout the paper and in all the momentum space computations in our code.

By applying (54) and some integrations by parts to our Ward identities, we get the momentum space transverse Ward identities, which are a set of algebraic constraints.

The momentum space $2T$ satisfies

$$p_{v_1} \langle T^{\mu_1 v_1}(p) T^{\mu_2 v_2}(-p) \rangle = 0. \tag{32}$$

For the three and four-point functions, the transverse Ward identities are quite cumbersome to write down fully expanded.

We present an expanded version of the first transverse Ward identity for the three-point function for illustration, whereas we keep the full sets given below implicit and refer the reader to Appendix A for a list of the explicit momentum space forms of the constituting elements

$$\begin{aligned} p_{1 v_1} \langle T^{\mu_1 v_1}(p_1) T^{\mu_2 v_2}(p_2) T^{\mu_3 v_3}(p_3) \rangle \\ = -p_3^{\mu_1} \langle T^{\mu_3 v_3}(p_2) T^{\mu_2 v_2}(-p_2) \rangle \\ - p_2^{\mu_1} \langle T^{\mu_2 v_2}(p_3) T^{\mu_3 v_3}(-p_3) \rangle \\ + p_3 v_1 \left[\delta^{\mu_1 v_3} \langle T^{v_1 \mu_3}(p_2) T^{\mu_2 v_2}(-p_2) \rangle \right. \\ \left. + \delta^{\mu_1 \mu_3} \langle T^{v_1 v_3}(p_2) T^{\mu_2 v_2}(-p_2) \rangle \right] \\ + p_2 v_1 \left[\delta^{\mu_1 v_2} \langle T^{v_1 \mu_2}(p_3) T^{\mu_3 v_3}(-p_3) \rangle \right. \\ \left. + \delta^{\mu_1 \mu_2} \langle T^{v_1 v_2}(p_3) T^{\mu_3 v_3}(-p_3) \rangle \right]. \end{aligned} \tag{33}$$

For every nT , there is of course one such Ward identity for each EMT. We present the full set here below for the three-point function in compact form,

$$\begin{aligned} p_{1 v_1} \langle T^{\mu_1 v_1}(p_1) T^{\mu_2 v_2}(p_2) T^{\mu_3 v_3}(p_3) \rangle \\ = -2i \left[\Gamma_{\kappa v_1}^{\mu_1} \right]^{\mu_2 v_2}(p_2) \langle T^{\kappa v_1}(p_3) T^{\mu_3 v_3}(-p_3) \rangle + (2 \leftrightarrow 3) \\ p_{2 v_2} \langle T^{\mu_1 v_1}(p_1) T^{\mu_2 v_2}(p_2) T^{\mu_3 v_3}(p_3) \rangle \\ = -2i \left[\Gamma_{\kappa v_2}^{\mu_2} \right]^{\mu_1 v_1}(p_1) \langle T^{\kappa v_2}(p_3) T^{\mu_3 v_3}(-p_3) \rangle + (1 \leftrightarrow 3) \\ p_{3 v_3} \langle T^{\mu_1 v_1}(p_1) T^{\mu_2 v_2}(p_2) T^{\mu_3 v_3}(p_3) \rangle \\ = -2i \left[\Gamma_{\kappa v_3}^{\mu_3} \right]^{\mu_1 v_1}(p_1) \langle T^{\kappa v_3}(p_2) T^{\mu_2 v_2}(-p_2) \rangle + (1 \leftrightarrow 2). \end{aligned} \tag{34}$$

Finally, for the four-point correlator we have 4 transverse Ward identities (this is the last set for which we report all channels; in what follows only one channel for every Ward identity will be explicitly written, though all of them were tested),

$$\begin{aligned} p_{1 v_1} \langle T^{\mu_1 v_1}(p_1) T^{\mu_2 v_2}(p_2) T^{\mu_3 v_3}(p_3) T^{\mu_4 v_4}(p_4) \rangle \\ = 2i \left[\Gamma_{\kappa v_1}^{\mu_1} \right]^{\mu_2 v_2}(p_2) \langle T^{\kappa v_1}(-p_3 - p_4) T^{\mu_3 v_3}(p_3) T^{\mu_4 v_4}(p_4) \rangle \\ - 2 \left[\Gamma_{\kappa v_1}^{\mu_1} \right]^{\mu_3 v_3 \mu_4 v_4}(p_3, p_4) \langle T^{\kappa v_1}(-p_2) T^{\mu_2 v_2}(p_2) \rangle + (2 \leftrightarrow 3, 2 \leftrightarrow 4), \\ p_{2 v_2} \langle T^{\mu_1 v_1}(p_1) T^{\mu_2 v_2}(p_2) T^{\mu_3 v_3}(p_3) T^{\mu_4 v_4}(p_4) \rangle \\ = 2i \left[\Gamma_{\kappa v_2}^{\mu_2} \right]^{\mu_1 v_1}(p_1) \langle T^{\kappa v_2}(-p_3 - p_4) T^{\mu_3 v_3}(p_3) T^{\mu_4 v_4}(p_4) \rangle \end{aligned}$$

$$\begin{aligned}
 & -2 \left[\Gamma_{\kappa\nu_2}^{\mu_2} \right]^{\mu_3\nu_3\mu_4\nu_4} (p_3, p_4) \langle T^{\kappa\nu_2}(-p_1) T^{\mu_1\nu_1}(p_1) \rangle + (1 \leftrightarrow 3, 1 \leftrightarrow 4) \Big], \\
 p_{3\nu_3} & < T^{\mu_1\nu_1}(p_1) T^{\mu_2\nu_2}(p_2) T^{\mu_3\nu_3}(p_3) T^{\mu_4\nu_4}(p_4) > \\
 & = 2i \left[\left[\Gamma_{\kappa\nu_3}^{\mu_3} \right]^{\mu_1\nu_1}(p_1) \langle T^{\kappa\nu_3}(-p_2 - p_4) T^{\mu_2\nu_2}(p_2) T^{\mu_4\nu_4}(p_4) \rangle \right. \\
 & \quad \left. - 2 \left[\Gamma_{\kappa\nu_3}^{\mu_3} \right]^{\mu_2\nu_2\mu_4\nu_4} (p_2, p_4) \langle T^{\kappa\nu_3}(-p_1) T^{\mu_1\nu_1}(p_1) \rangle + (1 \leftrightarrow 2, 1 \leftrightarrow 4) \right], \\
 p_{4\nu_4} & < T^{\mu_1\nu_1}(p_1) T^{\mu_2\nu_2}(p_2) T^{\mu_3\nu_3}(p_3) T^{\mu_4\nu_4}(p_4) > \\
 & = 2i \left[\left[\Gamma_{\kappa\nu_4}^{\mu_4} \right]^{\mu_1\nu_1}(p_1) \langle T^{\kappa\nu_4}(-p_2 - p_3) T^{\mu_2\nu_2}(p_2) T^{\mu_3\nu_3}(p_3) \rangle \right. \\
 & \quad \left. - 2 \left[\Gamma_{\kappa\nu_4}^{\mu_4} \right]^{\mu_2\nu_2\mu_3\nu_3} (p_2, p_3) \langle T^{\kappa\nu_4}(-p_1) T^{\mu_1\nu_1}(p_1) \rangle + (1 \leftrightarrow 2, 1 \leftrightarrow 3) \right]. \tag{35}
 \end{aligned}$$

Deriving the trace Ward identities is simpler. Rewriting (5) with $n_I = 1$ as

$$g_{\mu_1\nu_1} \frac{\delta \mathcal{W}}{\delta g_{\mu_1\nu_1}(x_1)} = \frac{\sqrt{g}}{2} \mathcal{A}[g], \tag{36}$$

we can functionally differentiate up to three more times and obtain, after Fourier-transforming to momentum space with (54),

$$\begin{aligned}
 \delta_{\mu_1\nu_1} & < T^{\mu_1\nu_1}(-p_1) T^{\mu_2\nu_2}(p_1) > \\
 & = \left[\sqrt{g}, \mathcal{A}[g] \right]^{\mu_2\nu_2}(p_1), \tag{37}
 \end{aligned}$$

$$\begin{aligned}
 \delta_{\mu_1\nu_1} & < T^{\mu_1\nu_1}(p_1) T^{\mu_2\nu_2}(p_2) T^{\mu_3\nu_3}(p_3) > \\
 & = \left[\sqrt{g}, \mathcal{A}[g] \right]^{\mu_2\nu_2\mu_3\nu_3}(p_2, p_3), \\
 & - < T^{\mu_2\nu_2}(-p_2) T^{\mu_3\nu_3}(p_2) > \\
 & - < T^{\mu_2\nu_2}(-p_3) T^{\mu_3\nu_3}(p_3) > \tag{38}
 \end{aligned}$$

$$\begin{aligned}
 \delta_{\mu_1\nu_1} & < T^{\mu_1\nu_1}(p_1) T^{\mu_2\nu_2}(p_2) T^{\mu_3\nu_3}(p_3) T^{\mu_4\nu_4}(p_4) > \\
 & = \left[\sqrt{g}, \mathcal{A}[g] \right]^{\mu_2\nu_2\mu_3\nu_3\mu_4\nu_4}(p_2, p_3, p_4), \\
 & - < T^{\mu_2\nu_2}(-p_3 - p_4) T^{\mu_3\nu_3}(p_3) T^{\mu_4\nu_4}(p_4) > \\
 & - < T^{\mu_3\nu_3}(-p_2 - p_4) T^{\mu_2\nu_2}(p_2) T^{\mu_4\nu_4}(p_4) > \\
 & - < T^{\mu_4\nu_4}(-p_2 - p_3) T^{\mu_2\nu_2}(p_2) T^{\mu_3\nu_3}(p_3) > . \tag{39}
 \end{aligned}$$

The structure of the anomalies for our correlators is implicitly given by

$$\begin{aligned}
 \left[\mathcal{A}[g] \right]^{\mu_2\nu_2}(p_2) & = -\frac{2}{3} \beta_a \left[\square R \right]^{\mu_2\nu_2}(p_2), \\
 \left[\mathcal{A}[g] \right]^{\mu_2\nu_2\mu_3\nu_3}(p_2, p_3) & \\
 & = \beta_a \left(\left[F \right]^{\mu_2\nu_2\mu_3\nu_3}(p_2, p_3) - \frac{2}{3} \left[\sqrt{g} \square R \right]^{\mu_2\nu_2\mu_3\nu_3}(p_2, p_3) \right) \\
 & \quad + \beta_b \left[G \right]^{\mu_2\nu_2\mu_3\nu_3}(p_2, p_3), \\
 \left[\mathcal{A}[g] \right]^{\mu_2\nu_2\mu_3\nu_3\mu_4\nu_4}(p_2, p_3, p_4) & \\
 & = \beta_a \left(\left[\sqrt{g} F \right]^{\mu_2\nu_2\mu_3\nu_3\mu_4\nu_4}(p_2, p_3, p_4) \right. \\
 & \quad \left. - \frac{2}{3} \left[\sqrt{g} \square R \right]^{\mu_2\nu_2\mu_3\nu_3\mu_4\nu_4}(p_2, p_3, p_4) \right) \\
 & \quad + \beta_b \left[\sqrt{g} G \right]^{\mu_2\nu_2\mu_3\nu_3\mu_4\nu_4}(p_2, p_3, p_4), \tag{40}
 \end{aligned}$$

whereas the explicit construction is available in the notebook *functional_derivatives.nb*. In the next section we discuss in detail their connection with 1 loop counterterms and how we can use the two for a preliminary test of our calculation of the four-point correlator with *Package-X*.

One comment about the anomaly is in order: since the term $\propto \square R$ can be removed by either adding an integral $\propto \int d^d x R^2$ [39] or by promoting the numerical coefficients in the Weyl counterterm to be functions of the spacetime dimension d [1], many an author choose to do so. Elsewhere we have discussed these issues in detail too [6], but we will not linger over it here. In this paper, we just perform the calculation in DR with no supplemental local counterterm, so that (9) is the correct generating functional for the trace anomaly of our correlators.

Finally, there are the Ward identities implied by special conformal transformations, but we will not deal with them in the present work. For a detailed discussion of the derivation and the solution of these identities for two and three-point functions, see [4].

4 Counterterms, anomalies and a preliminary test of the 4T correlator

In this section we review the derivation of the 1 loop counterterms for EMT correlators and we derive the Ward identities which they must satisfy and which connect them with the respective trace anomalies. We explicitly compute these counterterms and check all of the mentioned Ward identities. Since both the counterterms and the anomalies for the 4T correlator are highly non trivial structures, the successful check of these tests is a very strong indicator that their calculation is correct.

Therefore, if it is possible to evaluate only the ultraviolet pole of our four-point function, after putting together the tensor integrals corresponding to the diagrams of Sect. 2, we can compare it to the independently tested counterterm. If the two expressions match, we have a strong preliminary hint that the diagrams have been assembled correctly. We actually performed this test, as the *LoopIntegrate* routine of *Package-X*, which substitutes explicit expressions of scalar coefficients into tensor integrals, has an option for extracting only the ultraviolet pole of each scalar coefficient. Summing up the poles of all diagrams, we did match the rank-8 counterterm for the our correlator.

In order to be as self-contained as possible, we provide here the general formulas for the Passarino-Veltman coefficient functions we employ [40], so as to clarify the meaning of the symbols *PVB*, *PVC* and *PVD* that the reader will encounter in the snippets of code to follow and in the notebooks. In the following formula, the symbol r stands for the number of times the metric tensor enters in the symmetric

tensor multiplying the coefficient function, whereas n_1, n_2 and n_3 stand for the number of times each of the external momenta enters in it,

$$\begin{aligned}
 &PVB[r, n_1, s, m_0, m_1] \\
 &\equiv \underbrace{\mathbf{B}_{0 \dots 0}}_{2r} \underbrace{1 \dots 1}_{n_1}, \text{ coefficient of } \{[p_1]^{n_1} [g]^r\}^{\mu_1 \dots \mu_{2r+n_1}}, \\
 &PVC[r, n_1, n_2, s_1, s_{12}, s_2, m_0, m_1, m_2] \\
 &\equiv \underbrace{\mathbf{C}_{0 \dots 0}}_{2r} \underbrace{1 \dots 1}_{n_1} \underbrace{2 \dots 2}_{n_2}, \\
 &\text{coefficient of } \{[p_1]^{n_1} [p_2]^{n_2} [g]^r\}^{\mu_1 \dots \mu_{2r+n_1+n_2}}, \\
 &PVD[r, n_1, n_2, n_3, s_1, s_2, s_3, s_4, s_{12}, s_{23}, m_0, m_1, m_2, m_3] \\
 &\equiv \underbrace{\mathbf{D}_{0 \dots 0}}_{2r} \underbrace{1 \dots 1}_{n_1} \underbrace{2 \dots 2}_{n_2} \underbrace{3 \dots 3}_{n_3}, \\
 &\text{coefficient of } \{[p_1]^{n_1} [p_2]^{n_2} [p_3]^{n_3} [g]^r\}^{\mu_1 \dots \mu_{2r+n_1+n_2+n_3}}.
 \end{aligned} \tag{41}$$

The notebook *correlators_calculation.nb* presents the procedure for all of the EMT correlators through four-point, giving also plenty of details about the calculation of the whole correlators.³

The syntax of the routines employed in the code is the following (see Fig. 6):

- *LoopIntegrate* is the central routine of the package and performs the reduction of the tensor integrals. Its first argument is the numerator of the tensor integral, the second is the loop momentum, the following pair given as arguments have the structure (*mom, mass*) where *mom* is the momentum and *m* is the mass of the propagating particle for each propagator in the loops. The mass is always 0 for us. Various options can be given, for which we refer the reader to the *Package-X* guide, included in the *Mathematica* interactive documentation upon successful installation of the package.
- *LoopRefine* converts the Passarino-Veltman coefficient functions to analytic expressions which can be readily evaluated numerically, extracting the ultraviolet pole from the scalar two-point function. Various options can be given, among which is *Part* \rightarrow *UVdivergent*, which makes the routine extract only the ultraviolet pole of the expression; for other options we refer the reader to the *Package-X* guide.

In the following, we discuss in detail the 1 loop counterterms and the Ward identities they are subjected to. We refer the reader to the public repository for further details. This is actually not the first time that the four-point function

³ In the conventions of *Package-X*, one works in the \overline{MS} scheme and must think of $1/\epsilon$ as of $1/\epsilon - \gamma + \log(4\pi)$, γ being the Euler-Mascheroni constant.

```

In[ ]:= << X`
Package-X v2.1.1, by Hiren H. Patel
For more information, see the guide

In[ ]:= HoldForm[LoopIntegrate[1, l, {l, 0}, {l + p1, 0}]]
Out[ ]:=  $\int \frac{d^d l}{(2\pi)^d} \frac{1}{l^2 (l + p_1)^2}$ 

In[ ]:= scalcoeff = LoopIntegrate[1, l, {l, 0}, {l + p1, 0}]
Out[ ]:= PVB[0, 0, p1.p1, 0, 0]

In[ ]:= LoopRefine[scalcoeff]
Out[ ]:=  $2 + \frac{1}{\epsilon} + \text{Log}\left[-\frac{\mu^2}{p_1.p_1}\right]$ 

In[ ]:= LoopRefine[scalcoeff, Part -> UVDivergent]
Out[ ]:=  $\frac{1}{\epsilon}$ 
    
```

Fig. 6 Loading *Package-X* in *Mathematica* and extracting the UV pole of the scalar two-point function

counterterms were computed, as they were already worked out in [41], where their relation to the trace anomaly - to be discussed shortly - was exploited to explore dilaton interactions in the conformal limit of the Standard Model. Another application was explored in [42], where a recursive relation allowing to compute fully traced correlators of the energy-momentum tensor was discovered.

The term we add to the action in our generating functional \mathcal{W} in order to renormalize our (unrenormalizable) theory in (3) is the following,

$$S_{counter} = -\frac{\mu^{-2\epsilon}}{\epsilon} \int d^d x \sqrt{g} \left(\beta_a F + \beta_b G \right), \tag{42}$$

with $d = 4 - 2\epsilon$, containing the squared Weyl tensor F and the Euler density G , defined in Appendix A. Since the integral of the Euler density is a topological invariant for $d = 4$, it can be proven that the Euler part of the three and four-point counterterms derived from (42) are actually finite, because the functional derivatives of the integral of the Euler density in $d = 4 - 2\epsilon$ dimensions are $\propto \epsilon$. This means that the contribution subtracted through the term $\propto \beta_b$ in (42) is finite and, thus, this amounts to a choice of the renormalization scheme. To the best of our knowledge, this was first argued and shown to be true for $d = 2$ in [43], while a very detailed technical derivation in momentum space recently appeared in [5], to which we refer the interested reader, particularly for the case of the Euler counterterm of the three-point EMT correlation function in $d = 4$. The latter is studied in great detail on the grounds of an elegant form factor decomposition of the three-point correlator, which unveils the hidden dimension-dependent degeneracy underpinning the vanishing of the functional variations of the integrated Euler density

in 4 dimensions. On our side, since we do not have such a general decomposition of our four-point function at our disposal yet, we do not attempt the generalization of this procedure for the four-point function, but we employ another approach, discussed in Appendix A.2 of [4], to explicitly show the vanishing of the Euler counterterm for both the three and four-point functions in the notebook *vanishing_euler_ct.nb*, discussing the procedure in Appendix A.3. This explicitly proves that, also for the four-point function, the Euler contribution to the counterterm serves as a finite renormalization which has the ultimate purpose of yielding a correlator whose trace anomaly has the expected form (40).

The counterterm (42) could be further supplemented by additional and explicitly finite terms $\propto \beta_a$, but we chose not to include such a discussion, which can be found in many papers on EMT correlators [1, 6, 31].

For the general nT correlator, the counterterm action (42) generates the n -point vertex

$$-\frac{\mu^{-2\epsilon}}{\epsilon} \left(\beta_a D_F^{\mu_1 \nu_1 \dots \mu_n \nu_n}(x_1, \dots, x_n) + \beta_b D_G^{\mu_1 \nu_1 \dots \mu_n \nu_n}(x_1, \dots, x_n) \right), \tag{43}$$

where

$$D_F^{\mu_1 \nu_1 \dots \mu_n \nu_n}(x_1, \dots, x_n) = 2^n \frac{\delta^n}{\delta g_{\mu_1 \nu_1}(x_1) \dots \delta g_{\mu_n \nu_n}(x_n)} \int d^d x \sqrt{g} F, \tag{44}$$

$$D_G^{\mu_1 \nu_1 \dots \mu_n \nu_n}(x_1, \dots, x_n) = 2^n \frac{\delta^n}{\delta g_{\mu_1 \nu_1}(x_1) \dots \delta g_{\mu_n \nu_n}(x_n)} \int d^d x \sqrt{g} G. \tag{45}$$

The momentum space counterterms are defined via the same Fourier transform defining the momentum space correlation functions (54).

We have derived in detail the first functional variation of the integral of a general expression which is quadratic in the Riemann tensor in a shared appendix of [6, 31]. Here we provide only the final result.

Let $K = (a R^{\alpha\beta\gamma\delta} R_{\alpha\beta\gamma\delta} + b R^{\alpha\beta} R_{\alpha\beta} + c R^2)$, with a, b and c arbitrary real numbers; then

$$\begin{aligned} & \frac{\delta}{\delta g_{\mu_1 \nu_1}(x)} \int d^d x \sqrt{g} K \\ &= \sqrt{g} \left\{ \frac{1}{2} g^{\mu_1 \nu_1} K - 2a R^{\mu\alpha\beta\gamma} R^{\nu}_{\alpha\beta\gamma} \right. \\ & \quad + 4a R^{\mu_1 \alpha} R^{\nu}_{\alpha} - (4a + 2b) R^{\mu_1 \alpha \nu_1 \beta} R_{\alpha\beta} - 2c R R^{\mu_1 \nu_1} \\ & \quad + (4a + b) \square R^{\mu_1 \nu_1} + (4c + b) g^{\mu_1 \nu_1} R^{\alpha\beta}_{;\alpha;\beta} \\ & \quad \left. - (4a + 2b + 4c) R^{\nu_1 \beta}_{;\beta}{}^{\mu_1} \right\}. \tag{46} \end{aligned}$$

From the equation above, the counterterm action (42) and taking traces in d dimensions, since we are working in DR,

one can derive the trace anomaly observing that

$$\begin{aligned} g_{\mu_1 \nu_1}^{(d)} \frac{\delta}{\delta g_{\mu_1 \nu_1}(x)} \int d^d x \sqrt{g} F &= -\sqrt{g} \frac{\epsilon}{2} \left(F - \frac{2}{3} \square R \right), \\ g_{\mu_1 \nu_1}^{(d)} \frac{\delta}{\delta g_{\mu_1 \nu_1}(x)} \int d^d x \sqrt{g} G &= -\sqrt{g} \frac{\epsilon}{2} G, \end{aligned} \tag{47}$$

where we have distinguished the d -dimensional trace with a superscript on the metric tensor.

Using these expressions, the renormalized two, three and four-point correlators in momentum space can be written as

$$\begin{aligned} & \langle T^{\mu_1 \nu_1}(-p_2) T^{\mu_2 \nu_2}(p_2) \rangle_{ren} \\ &= \langle T^{\mu_1 \nu_1}(-p_2) T^{\mu_2 \nu_2}(p_2) \rangle_{bare} \\ & \quad - \frac{1}{\epsilon} \beta_a D_F^{\mu_1 \nu_1 \mu_2 \nu_2}(-p_2, p_2), \\ & \langle T^{\mu_1 \nu_1}(p_1) T^{\mu_2 \nu_2}(p_2) T^{\mu_3 \nu_3}(p_3) \rangle_{ren} \\ &= \langle T^{\mu_1 \nu_1}(p_1) T^{\mu_2 \nu_2}(p_2) T^{\mu_3 \nu_3}(p_3) \rangle_{bare} \\ & \quad - \frac{1}{\epsilon} \left(\beta_a D_F^{\mu_1 \nu_1 \mu_2 \nu_2 \mu_3 \nu_3}(p_1, p_2, p_3) \right. \\ & \quad \left. + \beta_b D_G^{\mu_1 \nu_1 \mu_2 \nu_2 \mu_3 \nu_3}(p_1, p_2, p_3) \right), \\ & \langle T^{\mu_1 \nu_1}(p_1) T^{\mu_2 \nu_2}(p_2) T^{\mu_3 \nu_3}(p_3) T^{\mu_4 \nu_4}(p_4) \rangle_{ren} \\ &= \langle T^{\mu_1 \nu_1}(p_1) T^{\mu_2 \nu_2}(p_2) T^{\mu_3 \nu_3}(p_3) T^{\mu_4 \nu_4}(p_4) \rangle_{bare} \\ & \quad - \frac{1}{\epsilon} \left(\beta_a D_F^{\mu_1 \nu_1 \mu_2 \nu_2 \mu_3 \nu_3 \mu_4 \nu_4}(p_1, p_2, p_3, p_4) \right. \\ & \quad \left. + \beta_b D_G^{\mu_1 \nu_1 \mu_2 \nu_2 \mu_3 \nu_3 \mu_4 \nu_4}(p_1, p_2, p_3, p_4) \right). \end{aligned} \tag{48}$$

From these relations and from (32) to (35) it is apparent that the counterterms are related to each other by the same transverse Ward identities relating the EMT correlators. One can also separately check these identities for Weyl and Euler counterterms just by writing them down and equating the coefficients of β_a and β_b . This is done in the second part of the file *functional_derivatives.nb*.

Anomalous Ward identities for our counterterms can be derived through up to three more functional derivatives of Eqs. (47), so that identities which are completely analogous to (37)–(39) emerge, the only difference being that now traces are taken in d dimensions. We report them separately for the Weyl and Euler counterterms in the first channel: of course analogous identities -obtained by proper permutations of indices and momenta- hold in all channels.

$$\begin{aligned} \delta_{\mu_1 \nu_1}^{(d)} D_F^{\mu_1 \nu_1 \mu_2 \nu_2}(-p_2, p_2) &= -\frac{\epsilon}{2} \frac{2}{3} [\square R]^{\mu_2 \nu_2}(p_2), \\ \delta_{\mu_1 \nu_1}^{(d)} D_G^{\mu_1 \nu_1 \mu_2 \nu_2}(-p_2, p_2) &= 0, \\ \delta_{\mu_1 \nu_1}^{(d)} D_F^{\mu_1 \nu_1 \mu_2 \nu_2 \mu_3 \nu_3}(p_1, p_2, p_3) \\ &= -D_F^{\mu_2 \nu_2 \mu_3 \nu_3}(-p_2, p_2) - D_F^{\mu_2 \nu_2 \mu_3 \nu_3}(-p_3, p_3) \\ & \quad - \frac{\epsilon}{2} \left[\left(F - \frac{2}{3} \sqrt{g} \square R \right) \right]^{\mu_2 \nu_2 \mu_3 \nu_3}(p_2, p_3), \end{aligned} \tag{49}$$

$$\begin{aligned} &\delta_{\mu_1\nu_1}^{(d)} D_G^{\mu_1\nu_1\mu_2\nu_2\mu_3\nu_3}(p_1, p_2, p_3) \\ &= -D_G^{\mu_2\nu_2\mu_3\nu_3}(-p_2, p_2) - D_G^{\mu_2\nu_2\mu_3\nu_3}(-p_3, p_3) \\ &\quad - \frac{\epsilon}{2} \left[G \right]^{\mu_2\nu_2\mu_3\nu_3}(p_2, p_3), \end{aligned} \tag{50}$$

$$\begin{aligned} &\delta_{\mu_1\nu_1}^{(d)} D_F^{\mu_1\nu_1\mu_2\nu_2\mu_3\nu_3\mu_4\nu_4}(p_1, p_2, p_3, p_4) \\ &= -2 D_F^{\mu_2\nu_2\mu_3\nu_3\mu_4\nu_4}(-p_3 - p_4, p_3, p_4) \\ &\quad -2 D_F^{\mu_2\nu_2\mu_3\nu_3\mu_4\nu_4}(-p_2 - p_4, p_2, p_4) \\ &\quad -2 D_F^{\mu_2\nu_2\mu_3\nu_3\mu_4\nu_4}(-p_2 - p_3, p_2, p_3), \\ &\quad - \frac{\epsilon}{2} \left(\left[\sqrt{g} F \right]^{\mu_2\nu_2\mu_3\nu_3\mu_4\nu_4}(p_2, p_3, p_4) \right. \\ &\quad \left. - \frac{2}{3} \left[\sqrt{g} \square R \right]^{\mu_2\nu_2\mu_3\nu_3\mu_4\nu_4}(p_2, p_3, p_4) \right) \end{aligned}$$

$$\begin{aligned} &\delta_{\mu_1\nu_1}^{(d)} D_G^{\mu_1\nu_1\mu_2\nu_2\mu_3\nu_3\mu_4\nu_4}(p_1, p_2, p_3, p_4) \\ &= -2 D_G^{\mu_2\nu_2\mu_3\nu_3\mu_4\nu_4}(-p_3 - p_4, p_3, p_4) \\ &\quad -2 D_G^{\mu_2\nu_2\mu_3\nu_3\mu_4\nu_4}(-p_2 - p_4, p_2, p_4) \\ &\quad -2 D_G^{\mu_2\nu_2\mu_3\nu_3\mu_4\nu_4}(-p_2 - p_3, p_2, p_3) \\ &\quad - \frac{\epsilon}{2} \left[\sqrt{g} G \right]^{\mu_2\nu_2\mu_3\nu_3\mu_4\nu_4}(p_2, p_3, p_4). \end{aligned} \tag{51}$$

It is apparent that all these constraints are not trivial to satisfy. We checked all of them for all anomalies and counterterms and, thus, ensured that these were correctly computed.

As mentioned before, the ultraviolet pole of our four-point function is found to coincide with the overall counterterm for the scalar field $4T$.

The reason why we perform this preliminary check is twofold.

- The ultraviolet pole of our four-point function is highly non trivial, since there are 16 diagrams contributing to it, so that getting it right is a solid first check of the diagrammatic expansion. Beside, being a polynomial in the external momenta, the ultraviolet pole of our four-point function is much more manageable than the whole correlator, which requires much more memory and computing time. This makes it an ideal tool to quickly scan for potential mistakes in the Feynman expansion.
- The trace Ward identities connect the counterterms to the trace anomalies and, so, are a test for the latter as well. The trace anomalies are present also in turn in the trace Ward identities for the correlation functions (37)–(39), which we must test in order to ensure the correctness of the four-point function. Thus, having them tested in advance reassures us about the correctness of the trace identities, so that any mismatch emerging from them can be quite surely traced back to the four-point function.

One last comment is in order. The Euler characteristic -the integral over all space of the Euler density- is topologically invariant, i.e. it does not depend on the specific metric tensor

used in the integrand, so its derivatives w.r.t. the metric vanish identically for $d = 4$, meaning they are $\propto \epsilon$ in $d = 4 - 2\epsilon$, as already discussed below Eq. (42). Thus, checking that its functional derivatives correctly contribute to our counterterms because they remove terms $\propto 1/\epsilon$ in our regularized correlator effectively amounts to testing that two finite sets of terms, one in the regularized correlator and the other in the counterterm, exactly match. Though our computer algebra stays “unaware” of the finiteness of these contributions, since the proportionality to ϵ is hidden, this is clearly a sensible test.

Once all these preliminary tests have been successful, we can be reasonably confident about the diagrammatic expansion. What is left is the computation of the whole four-point function and the test of the transverse and trace Ward identities. Plenty of details are available in the files *correlators_calculation.nb* and *ward_identities.nb*.

The purpose of the following section is to go into the necessary technical details about the calculation.

5 Into the full calculation

It is time to illustrate in detail how we employ our tools to nail down the whole four-point function. In the first part of this section we review the Feynman diagram computation, in the next two we give a survey of the checks of the Ward identities. A few snippets of code are provided in this section, but we encourage the interested reader to explore the notebooks, which are documented in great and hopefully sufficient detail.

5.1 The calculation of the four-point correlator

The calculation is performed by the file *correlators_calculation.nb*. The code employs *Package-X* to automate the Passarino-Veltman reduction of the many tensor integrals one encounters.

The notebook starts by loading the vertices and counterterms stored in the *all_functional_derivatives* file, which must be generated beforehand by running *functional_derivatives.nb*. After that, the notebook is divided into three parts, one for each of the three computed correlators. The structure of these three parts is similar and unfolds as follows.

- The numerators of the contributing Feynman diagrams are constructed. As detailed in Sect. 2, there is only 1 for the $2T$, while there are 4 for the $3T$ and 16 for the $4T$. An image of each computed diagram is loaded in the notebook right before the line computing its numerator. In the case of the two-point function, the known result for general values of the improvement parameter (see Eq. 10) is presented and rederived for the reader’s convenience.

The case with $\chi = 1/6$ corresponds to the conformally invariant case and is eventually selected.⁴

- The *LoopIntegrate* routine is invoked to perform the tensor reduction of the diagrams. For the three bubbles in the three-point function and for all the diagrams contributing to the four-point function, only blueprint diagrams with generic momenta are computed. The actual diagrams are obtained by replacing the generic momenta with the sets classified in Sect. 2. This is topical for the four-point function, due to the memory it requires (see next point).
- The *LoopRefine* routine is employed to extract the ultraviolet poles from each diagram and to sum them up in order to identify the ultraviolet divergence of the correlator. This is then compared to the corresponding counterterm and exact matching is found, so the whole correlators are stored in the files *T2_scalar*, *T3_scalar* and *T4_scalar*. The first two contain just the full two and three-point correlators, whereas *T4_scalar* stores only the four blueprint diagrams, because of the amount of memory the full result would otherwise require: the blueprint for the square diagram takes roughly 2.3 GB of memory by itself. This is before substituting an explicit set of momenta, which makes it even lengthier because some of them are the sum of more momenta and before exploiting the momentum conservation constraint $p_1 \rightarrow -(p_2 + p_3 + p_4)$.

The results presented in this section were relatively straightforward to get, although one of them requires quite some time: the extraction of the ultraviolet pole of the square diagram contributing to the four-point function takes roughly 20 mins even when parallelized among 8 kernels, each one running on a different core of a 2,4 GHz Intel Core i9 CPU. Nevertheless, despite the time required, the amount of memory used to accomplish any of the tasks in this notebook never exceeds 4 GB, which makes it easy to execute on any modern laptop.

Unfortunately, this is not the case for the tests of the Ward identities for the *4T* correlator, as we will explain in a while. The next two sections deal with the content of the file *ward_identities.nb*.

5.2 Analytical checks of the Ward identities for the *2T* and *3T*

Checking the transverse and trace Ward identities for the two-point function, Eqs. (32) and (37), is trivial. The first two lines in Fig. 7 should be self explanatory, once the reader has understood the essential purpose of the *LoopRefine* routine explained in Sect. 4 and that the **A2** object is just the anomaly on the rhs of (37).

⁴ See also the paragraph just before Sect. 2.1 about the choice $\chi = 1/6$ vs the general case $\chi = 1/4(d - 2)/(d - 1)$.

It is time to explain how to check the naive scaling dimension of the correlators. The underpinning idea is very simple. This dimension is called naive because proper scaling accounts for the effect of logarithms dependent on the ultraviolet scale $\propto \log(p^2/\mu^2)$, which come from the two-point scalar integrals. Since every term in our EMT correlators must be of dimension (*momentum*)⁴, we can replace it with its dimension, which we choose to denote with λ in the code. So, for instance, $p_\mu \rightarrow \lambda, g_{\mu\nu} \rightarrow \lambda^0$. Once all the replacements have gone through, we expect to get just a real number times λ^4 , which is what is shown in the last input line of the snippet below and what is found for the higher-point functions as well.

One might ask why we do not undertake a check of the full dilatation identity, which would be, in $d = 4$, something like

$$\left(4 - \sum_{i=1}^n p_i^\lambda \frac{\partial}{\partial p_i^\lambda}\right) \langle T^{\mu_1\nu_1}(p_1) \dots T^{\mu_n\nu_n}(p_n) \rangle = \text{anomalous terms.} \tag{52}$$

The reason is that checking the trace identities (37)–(39) already implies satisfying the scale invariance requirement. Indeed, the trace anomaly equation (5) is obtained by studying the transformation of the generating functional of a field theory embedded in curved space under a local rescaling of the metric tensor, which is called a Weyl transformation. This is a more general transformation than a global rescaling of coordinates and, for Lagrangian field theories which are at most quadratic in their fields derivatives, is effectively equivalent to full-fledged conformal invariance [32]. This means in turn that, since this symmetry is broken only by the trace anomaly, which can be seen as a by-product of the ultraviolet renormalization of the EMT, it follows that, if an EMT correlator satisfies its anomalous trace identity, the correlator must also be scale invariant in the sense of (52). In particular this implies that, if its momenta are uniformly rescaled by a global factor $p \rightarrow \lambda p$, it must change by an overall factor λ^4 plus additional contributions due to the logarithms associated to the regularization scale μ^2 , introduced to consistently regularize ultraviolet divergencies $\propto \log(p^2/\mu^2) \rightarrow \log(p^2/\mu^2) + \log \lambda^2$. These are the contributions that, acted upon by the differential operators in Eq. (52), would render the anomalous term on the rhs. The fact that in Fig. 7 we are just checking the naive scale dimension is due to the replacement of the two-point scalar integrals with λ^0 , which does not take into account the logarithmic contribution.

Now, the reason why we are discussing the naive scale identity is that its check can be done analytically also for the complicated four-point correlator and, as such, will prove very useful in the last part of this section, when numerical stability of our results is discussed.


```

In[*]:= p2.v2 T2[μ1, ν1, μ2, ν2, p2] // Contract // LoopRefine
Out[*]:= 0

In[*]:= (T2[μ1, ν1, μ2, ν2, p2] /. {gμ1,ν1 → 4} /. {μ1 → ν1} // Contract // LoopRefine) -
        2 A2[μ2, ν2, p2, βa] // Simplify
Out[*]:= 0

In[*]:= T2[μ1, ν1, μ2, ν2, p2] /. {d → 4} /. {LDot[a_, b_] :=> λ^2} /. {PVB[n_, x___] :=> λ^2^n} /.
        {LTensor[MetricG, μ_, ν_] :=> 1} /. {LTensor[p_, μ_] → λ}
Out[*]:= 17 λ^4 / 32 π^2

```

Fig. 7 Check of the transverse and trace Ward identities as well as of the naive scaling dimension for the two-point function

Next we come to the tests of the Ward identities for the three-point function, which is more involved but was already done in [6] in pretty much the same way, which we reproduce here. The idea behind the procedure for both transverse and trace identities is the same and quite simple.

- Load the tensor basis which spans the space of rank-5 or rank-4 tensors dependent on 2 independent momenta to which belongs the correlator contracted with the momentum in (34) or with the metric tensor in (38); assign to them the correct indices (those which survive after contraction).
- Build the lhs and rhs for each Ward identity separately.
- Isolate the coefficients of each tensor in the basis for both the lhs and the rhs, subtract them from each other and check that for all of them the result is zero.

We have checked all three transverse identities (34) and trace identities (38). For further details, the reader is encouraged to look at the code, where she will also encounter the *KallenExpand* routine, which plugs the explicit expression for the Källén polynomial $\lambda(a, b, c) = a^2 + b^2 + c^2 - 2ab - 2ac - 2bc$ in place of its symbolic representation.

5.3 Numerical checks of the Ward identities for the $4T$ correlator

This is the most slippery and time consuming part of our project, because the whole $4T$ correlator is just too big to be dealt with analytically within reasonable time with an ordinary computer, even one with a $64GB$ RAM like the one at our disposal. As we mentioned above, the blueprint of the square diagrams contributing to the $4T$ are the culprits, each one of them occupying alone almost $4GB$ of memory space after the proper momenta assignments. These assignments are such that the second argument of each diagram is the sum of two external momenta (see the notebook and the diagrams of

Sect. 2) which, considering the amount of terms it consists of, significantly increases the necessary memory. The first feature which is required from the needed computer is quite some RAM: at least 40 available GB, in order for the computation not to crush. The second crucial feature is to have more than one available CPU core to perform calculations, in order to reduce the required time to a reasonable window through parallelization. In our case, we had 8 kernels and a $64GB$ RAM at our disposal on our machine, which allowed us to complete the test of all the 9 Ward identities for the $4T$ correlator in slightly less than 1 h.⁵

In order to speed up our numerical effort, we resorted to the *CollierLink* package, which connects *Package-X* with the *COLLIER* library (written in C language) in order to provide fast numerical evaluation of the scalar integrals. A fundamental component of the numerical evaluation procedure is to isolate the ultraviolet poles from the rest of the correlators.

The steps of the testing procedure explained for the $3T$ Ward identities hold here as well, with two caveats. First, the tensor bases to be used are now much bigger, due to the increased number of indices from 5 to 7 for transverse Ward identities and from 4 to 6 for trace Ward identities, beside the fact that we have one more independent momentum in our correlator w.r.t. the three-point case; second, the matching of the coefficients must now be checked numerically in order to guarantee sufficient speed and, for most common computers, not to crush.

On the ground of what was explained so far, one might think that subtracting the counterterm for the $4T$ after applying the *LoopRefine* routine to the computed correlator -even parallelizing it- would do the job: it would indeed, but that would be much too slow.

⁵ We are perfectly aware that state-of-the-art numerical calculations, e.g. for multiloop LHC phenomenology, require tens of thousands of CPU hours to complete, dwarfing our case. The spirit of our endeavor is different though: we are ultimately after some clever way to handle these results on even less powerful devices than ours in a near future.

What one can do, instead, is to resort to *CollierLink*, which can perform direct numerical evaluation of the Passarino-Veltman coefficient functions bypassing the analytic expansion. The task is parallelized in the notebook through the *ParallelMap Mathematica* routine, which distributes the task among the various available kernels. The parallelized task is in turn a sequence of two steps.

- The *SeparateUV* routine of *CollierLink* isolates the UV pole in each coefficient function.
- The *numrep* set of rules, defined above in the notebook, replaces all the scalar products of momenta with the corresponding numerical values obtained after choosing a completely off-shell configuration which respects $p_1 + p_2 + p_3 + p_4 = 0$. The input of numerical values into the scalar integrals automatically triggers *CollierLink* to invoke the COLLIER library and to evaluate the scalar coefficients numerically. We must specify a few things in order to have *CollierLink* run as we need, such as the accuracy required in the evaluation of scalar integrals, which we set to 10^{-10} ⁶, and the maximum tensor rank of our integrals, 8. The ultraviolet regularization scale μ is set by default to 1, but this value can be changed (see the next part of this section).

This step is the real bottleneck of the whole procedure, for it takes $\simeq 40$ min to complete for most of the momenta configurations we have tested, which are

$$[p_1, p_2, p_3, p_4] = \begin{cases} [(5, -3, 0, 3), (-1, 1, 0, 1), (-2, 1, 0, -1), (-2, 1, 0, -1)] \\ [(-2, -3, 9, 1), (1, 2, 4, 1), (3, -6, -2, 0), (-2, 7, -11, -2)] \\ [(1, 1, 1, 1), (1, -1, -1, -1), (-1, \frac{1}{2}, \frac{1}{2}, \frac{1}{2}), (-1, -\frac{1}{2}, -\frac{1}{2}, -\frac{1}{2})] \\ \left(\frac{1}{\sqrt{2}} - \frac{1}{\sqrt{3}}\right) \times [(1, 1, 1, 1), (1, -1, -1, -1), (-1, \frac{1}{2}, \frac{1}{2}, \frac{1}{2}), (-1, -\frac{1}{2}, -\frac{1}{2}, -\frac{1}{2})] \end{cases} \quad (53)$$

Please notice that the fourth configuration is given by the momenta in the third one rescaled by the prefactor in round brackets. This will be topical for the upcoming discussion of the numerical precision and stability of the tests.

Once the numerical evaluation of the scalar coefficients has been performed, what is left in order to test the Ward identities is to contract the listed diagrams with either one of the momenta or the metric tensor, perform the few more numerical replacements on the scalar products this produces, perform the same operations on the corresponding rhs (see Eqs. 35 and 39) and compare the scalar coefficients one by one. Then, if all the differences are acceptably small, we can declare the test successful. The corresponding snippet of code is given in Fig. 8, which we comment below

⁶ This is 2 orders of magnitude smaller than the precision required for the numerical test, 10^{-8} .

- *lhscov1* is the lhs of (35) and the set of rules in the curly brackets are the (faster) equivalent of the contraction with the p_1 momentum. When momentum conservation is employed at the end, it can affect only tensor structures, as it must in order not to miss any terms, since the tensor basis *tens371* depends only on 3 independent momenta.
- *rhscov1* is the rhs of Eq. (35), the Γ_1 and Γ_2 symbols being defined in Appendix B, whereas the T_2 and the T_3 functions are obviously the two and three-point correlators.
- *checkcov1* is a table, evaluated in parallel, made up by the differences of all scalar coefficients of the lhs and the rhs over the basis of rank 7 tensors with 3 independent momenta. The additional function *Labeled* just marks every difference with the number of the tensor in the list, which could be needed after an unsuccessful test to track down the tensors whose coefficients on the lhs and rhs of the identity do not match.
- The final line simply removes from the list all those numbers which were set equal to 0 through the *Chop* routine, because both their real and imaginary parts were under the *prec* threshold, which we set to 10^{-8} for the first three momentum configurations listed in (53). A dedicated discussion of the fourth momentum configuration, for which the precision threshold we manage to reach is not even close, being just 10^{-1} , aims at proving that this is definitely an expected issue of numerical instability. To this

end, the fact that we can easily check analytically naive scaling dimension is useful.

5.4 Discussion about numerical stability

The last point we wish to discuss before coming to our conclusions is the issue of numerical stability, which is raised when one tries to check the four-point functions Ward identities for momenta configurations like the last one in (53), which was purportedly chosen to be a rescaled version of the back-to-back third configuration, for which the test is precise through 8 decimal figures, just as for the former 3 as well.

This is when the test of the naive scale invariance of our correlators comes in handy, as we finally explain, reassuring us that the problem is only due to numerical instability. Now, the naive scaling dimension of every EMT correlator

```

In[•]:= lhscov1 = Plus@@ParallelMap[
  # /. {LTensor[x_, v1] := LDot[x, p1]} /. {LTensor[_Symbol, x_, v1] :=>
    LTensor[p1, x], LTensor[_Symbol, v1, x_] :=> LTensor[p1, x]} /. numrep &,
  t4list, Method -> "CoarsestGrained" /. {p1 -> -p2 - p3 - p4} // Expand;

In[•]:= rhscov1 =
  - (I (2 Γ1[μ2, v2, μ1, v1, κ, p2] × T3[κ, v1, μ3, v3, μ4, v4, p3, p4] + 2 Γ1[μ3, v3,
    μ1, v1, κ, p3] × T3[κ, v1, μ2, v2, μ4, v4, p2, p4] +
    2 Γ1[μ4, v4, μ1, v1, κ, p4] × T3[κ, v1, μ2, v2, μ3, v3, p2, p3] +
    4 Γ2[μ2, v2, μ3, v3, μ1, v1, κ, p2, p3] × T2[κ, v1, μ4, v4, p4] +
    4 Γ2[μ3, v3, μ4, v4, μ1, v1, κ, p3, p4] × T2[κ, v1, μ2, v2, p2] +
    4 Γ2[μ2, v2, μ4, v4, μ1, v1, κ, p2, p4] × T2[κ, v1, μ3, v3, p3]) //
  Contract // Expand // SeparateUV) /. numrep;

In[•]:= checkcov1 =
  ParallelTable[Labeled[Coefficient[lhscov1 - rhscov1, tens371[[i]]], i],
    {i, Length[tens37]}, Method -> "CoarsestGrained"];

In[•]:= DeleteCases[Chop[#, prec] &[checkcov1], Labeled[0, _]]

Out[•]:= {}

```

Fig. 8 Parallelized numerical comparison of the scalar coefficients over all the tensors in the base *tens371* (3 momenta, rank 7, indices assignments for the 1st identity) of the lhs and rhs of the first transverse

is (*momentum*)⁴, as one can see analytically for all correlators. This means that both the lhs and the rhs of every identity in (35) and (39) should naively scale by the same factor λ . To be completely precise, one must not forget to take into account the logarithmic contributions associated with scalar two-point functions which, as mentioned in Sect. 3, behave under rescaling like $\log(p^2/\mu^2) \rightarrow \log(\lambda^2 p^2/\mu^2) = \log(p^2/\mu^2) + \log \lambda^2$.

If it comes to numerically checking the rescaled identities, we can take care of this problem in two ways:

- by rescaling the regularization scale as well by $\mu \rightarrow \lambda\mu$, using the dedicated initialization option of the *Collier-Link* package: the snippet of code in Fig. 9 illustrates the invariance of the two-point function after rescaling both the momentum and the regularization scale.
- by leaving everything as it is, since the same two-point functions are present on both the lhs and rhs of the Ward identity, so that extra terms should coincide as well.

This proves that, if the identities are satisfied for a given momentum configuration, they should be identically satisfied for the rescaled configuration as well. Testing both possibilities is useful to realize that the extra logs coming from the rescaling of the momenta are not the source of the numerical instability. Indeed, what we find for our fourth momentum configuration, whether we take care of μ in the first way suggested above or not, is that the precision up to which the

Ward identity in (35). If smaller than the threshold $prec = 10^{-8}$ parameter, the result is subsequently chopped out of the list. The final result is an empty list, so the test is successful

Ward identity is numerically satisfied does not exceed 10^{-1} for some scalar coefficients in the tensor bases.

Nevertheless, since we proved that this result must vanish exactly too, the fact that the numerical agreement is excellent for such diverse momenta configurations as the first three leads us to the conclusion that our calculation is correct, although its numerical evaluation suffers from numerical instability, which is nevertheless to be expected for such huge expressions.

Of course, one can think of ways to improve our numerical tests.

The naive way could be to pursue a brute force approach: one would feed the numerical routines higher and higher precision inputs (*Mathematica* can numerically evaluate exact numbers to arbitrary numerical precision), but this would take an even heavier toll on the memory of the machine, which is already quite stretched with the required accuracy standards. A batch of several machines on which we could parallelize our numerical tests could do the job, of course. We do not have access to an integrated *Mathematica* deployment of this kind, but we firmly believe that the discussion above has clarified that this would add neither any further understanding nor improvement to our result, not least because, once one has a much higher available computing power, the identities could be tested analytically right off the bat.

A second way to go could be to compile our output into optimized *C++* or *Fortran* code. This is presumably feasible, but it goes behind the scope of the present work.

```

In[•]:= SetCollierLinkOptions[{"MuUV" → 1.}];

In[•]:= λ = 2.;

In[•]:= HoldForm[LoopIntegrate[1, l, {l, 0}, {l + p, 0}]]
Out[•]:= 
$$\int \frac{d^d l}{(2\pi)^d} \frac{1}{l^2 (l+p)^2}$$


In[•]:= LoopIntegrate[1, l, {l, 0}, {l + p1, 0}] /. {p1.p1 → 4.}
Out[•]:= 0.6137056389 + 3.141592654 i

In[•]:= SetCollierLinkOptions[{"MuUV" → 2.}];

In[•]:= LoopIntegrate[1, l, {l, 0}, {l + p1, 0}] /. {p1.p1 → λ^2 4.}
Out[•]:= 0.6137056389 + 3.141592654 i

```

Fig. 9 The scaling behaviour of the two-point function: scaling the regularization scale by the same factor as the momentum makes it behave as if its scaling dimension were the naive one, i.e. 0

These problems will stay, of course, only until a more clever way to compute the four-point function correlator is devised, which can yield a more compact result cutting off all the redundancies our method necessarily implies, but for the time being we consider ourselves satisfied.

6 Conclusions and perspectives

We have computed the four-point correlation function of the energy-momentum tensor in momentum space and provided a set of tools which allow the interested reader to reproduce the perturbative computation of the two, three and four-point correlation functions, together with the explicit and detailed construction of counterterms and anomalies and the test of the transverse and trace Ward identities. The results for the correlators are fully analytical, expressed in terms of Passarino-Veltman coefficient functions which can be easily either fully reduced to scalar integrals or evaluated numerically to arbitrary precision.

Considering the sheer dimension of our results, the main purpose of this work should be understood as the delivery of a benchmark for numerical checks of more compact results to be obtained in the future with different strategies, most probably the conformal bootstrap for fields with spin.

It would also be interesting to perform the same calculation for other Lagrangian conformal field theories, such as a fermion or a gauge field: actually, we already did this, but decided not to publish these results because they are even more massive than the scalar case and checking the Ward identities for the corresponding four-point correlation functions is computationally even more demanding. Furthermore,

unlikely the case of the three-point function, the results for the scalar, fermion and gauge fields do not allow to account for the full set of constants which would suffice to reconstruct any four-point correlator, so one does not gain much further insight into the structure of the CFT by computing them. Anyway, should we make progress on speeding up such checks, we will certainly update our repository.

Given the result by Dymarsky [18], it would be also very useful to identify the 22 independent structures making up the $4T$ correlation function in 4d in momentum space, perhaps after successfully accomplishing the task in 3d, where the number of independent structures is just 5. Once and if this task is accomplished, it would also be interesting to check the expected one-to-one correspondence between the momentum space result and the coordinate space results of [19–23]. The mapping between correlators in coordinate and momentum space has been investigated in some detail in [6,31] and shown to lead to some non trivial consistency conditions, which make this effort worth a separate work.

Also checking conformal Ward identities for our four-point correlator in momentum space would be interesting, but the task requires the implementation of second order differential operators and their application to a very complicated object. Since the Ward identities for the four-point correlator we did test were manageable only numerically, which was already a highly non trivial task, we did not try to figure out a way to perform the same numerical task as efficiently when working with differential operators, not least because our perturbative results for the lower point functions were shown in [7] to coincide with the non perturbative results of [4,5]. The latter were obtained by solving the full set of conformal Ward identities, so the work of implementing dif-

ferential operators in our codes for the three-point function without being able to extend the procedure to the four-point function would have added no original output to our effort. Again, should we make progress on this point, we will update our repository.

Acknowledgements First, I would like to sincerely thank Krzysztof Kutak for his support throughout the development of this project. I am very grateful to Hiren Patel for sharing insightful suggestions about *Package-X*, to Andreas van Hameren for pointing it to my attention and for making several useful comments about the numerical tests. Special thanks go to Misha Lublinsky for allowing me to deploy this computation on a powerful computer of the Ben Gurion University of the Negev. Useful discussions with Claudio Corianò and Matteo Maria Maglio are also gratefully acknowledged.

Data Availability Statement This manuscript has associated data in a data repository. [Authors' comment: The repository can be found and downloaded at <https://github.com/mirkos86/4-EMT-correlation-function-in-a-4d-CFT>. At the time this paper goes to print, it was last updated on June 20th, 2020.]

Open Access This article is licensed under a Creative Commons Attribution 4.0 International License, which permits use, sharing, adaptation, distribution and reproduction in any medium or format, as long as you give appropriate credit to the original author(s) and the source, provide a link to the Creative Commons licence, and indicate if changes were made. The images or other third party material in this article are included in the article's Creative Commons licence, unless indicated otherwise in a credit line to the material. If material is not included in the article's Creative Commons licence and your intended use is not permitted by statutory regulation or exceeds the permitted use, you will need to obtain permission directly from the copyright holder. To view a copy of this licence, visit <http://creativecommons.org/licenses/by/4.0/>.
Funded by SCOAP³.

A Conventions

A.1 Conventions for signs and momentum space correlators definition

The definition of the Fourier transform of the correlation function of n EMT's, which holds for any other n -point coordinate space function as well, is given by

$$\int d^d x_1 \dots d^d x_n \langle T^{\mu_1 \nu_1}(x_1) \dots T^{\mu_n \nu_n}(x_n) \rangle e^{-i(p_1 \cdot x_1 + \dots + p_n \cdot x_n)} = (2\pi)^d \delta^{(d)} \left(\sum_{i=1}^n k_i \right) \langle T^{\mu_1 \nu_1}(p_1) \dots T^{\mu_n \nu_n}(p_n) \rangle, \tag{54}$$

where all the momenta are conventionally taken to be incoming.

The covariant derivatives of a contravariant vector A^μ and of a covariant one B_μ are respectively

$$\nabla_\nu A^\mu \equiv \partial_\nu A^\mu + \Gamma_{\nu\rho}^\mu A^\rho \tag{55}$$

$$\nabla_\nu B_\mu \equiv \partial_\nu B_\mu - \Gamma_{\nu\mu}^\rho B_\rho, \tag{56}$$

with the Christoffel symbols defined as

$$\Gamma_{\beta\gamma}^\alpha = \frac{1}{2} g^{\alpha\kappa} [-\partial_\kappa g_{\beta\gamma} + \partial_\beta g_{\kappa\gamma} + \partial_\gamma g_{\kappa\beta}]. \tag{57}$$

Our definition of the Riemann tensor is

$$R^\lambda{}_{\mu\kappa\nu} = \partial_\nu \Gamma_{\mu\kappa}^\lambda - \partial_\kappa \Gamma_{\mu\nu}^\lambda + \Gamma_{\nu\eta}^\lambda \Gamma_{\mu\kappa}^\eta - \Gamma_{\kappa\eta}^\lambda \Gamma_{\mu\nu}^\eta. \tag{58}$$

The Ricci tensor is defined by the contraction $R_{\mu\nu} = R^\lambda{}_{\mu\lambda\nu}$ and the scalar curvature by $R = g^{\mu\nu} R_{\mu\nu}$.

The functional variations with respect to the metric tensor are computed using the relations

$$\begin{aligned} \delta\sqrt{g} &= -\frac{1}{2}\sqrt{g} g_{\alpha\beta} \delta g^{\alpha\beta} \\ \delta\sqrt{g} &= \frac{1}{2}\sqrt{g} g^{\alpha\beta} \delta g_{\alpha\beta} \\ \delta g_{\mu\nu} &= -g_{\mu\alpha} g_{\nu\beta} \delta g^{\alpha\beta} \\ \delta g^{\mu\nu} &= -g^{\mu\alpha} g^{\nu\beta} \delta g_{\alpha\beta}. \end{aligned} \tag{59}$$

The variations of the Christoffel symbols w.r.t. variations of the metric tensor are tensors themselves and their expression is

$$\begin{aligned} \delta\Gamma_{\beta\gamma}^\alpha &= \frac{1}{2} g^{\alpha\lambda} [-\nabla_\lambda(\delta g_{\beta\gamma}) + \nabla_\gamma(\delta g_{\beta\lambda}) + \nabla_\beta(\delta g_{\gamma\lambda})], \\ \nabla_\rho \delta\Gamma_{\beta\gamma}^\alpha &= \frac{1}{2} g^{\alpha\lambda} [-\nabla_\rho \nabla_\lambda(\delta g_{\beta\gamma}) + \nabla_\rho \nabla_\gamma(\delta g_{\beta\lambda}) + \nabla_\rho \nabla_\beta(\delta g_{\gamma\lambda})]. \end{aligned} \tag{60}$$

A.2 Weyl invariant and Euler density in 4d

It is well known that the object one has to deal with in order to construct Weyl-invariant objects for general dimensions d is the traceless part of the Riemann tensor, called the Weyl tensor, defined by

$$\begin{aligned} C_{\alpha\beta\gamma\delta} &= R_{\alpha\beta\gamma\delta} - \frac{1}{d-2}(g_{\alpha\gamma} R_{\delta\beta} + g_{\alpha\delta} R_{\gamma\beta} - g_{\beta\gamma} R_{\delta\alpha} - g_{\beta\delta} R_{\gamma\alpha}) \\ &\quad + \frac{1}{(d-1)(d-2)}(g_{\alpha\gamma} g_{\delta\beta} + g_{\alpha\delta} g_{\gamma\beta})R. \end{aligned} \tag{61}$$

This object enjoys the same symmetry properties of the Riemann tensor, i.e.

$$C_{\alpha\beta\gamma\delta} = -C_{\beta\alpha\gamma\delta} = C_{\beta\alpha\delta\gamma} = C_{\delta\gamma\beta\alpha}, \tag{62}$$

and, moreover, is traceless with respect to any couple of its indices. It is invariant under Weyl scalings of the metric

$$\delta_W C^\alpha{}_{\beta\gamma\delta} = 0. \tag{63}$$

In 4 dimensions, the only quantity which is Weyl invariant when multiplied by \sqrt{g} , is the Weyl tensor squared, which is

$$F \equiv C^{\alpha\beta\gamma\delta} C_{\alpha\beta\gamma\delta} = R^{\alpha\beta\gamma\delta} R_{\alpha\beta\gamma\delta} - 2 R^{\alpha\beta} R_{\alpha\beta} + \frac{1}{3} R^2. \tag{64}$$

The other quantity with which one can construct an integral which is Weyl invariant (in fact, a constant) for general even dimensions $d = 2k$ is the Euler density, defined as

$$E_{2k} = \frac{1}{2^k} \delta_{\mu_1 a_1 \nu_1 b_1 \dots \mu_k a_k \nu_k b_k} R^{\mu_1 \nu_1 \lambda_1 \kappa_1} \dots R^{\mu_k \nu_k a_k b_k}. \quad (65)$$

The antisymmetric Kronecker symbol is given by

$$\delta_{\nu_1 a_1 \nu_2 a_2 \dots \nu_n a_n} = n! \sum_{\mathcal{P}(a_1, \dots, a_n)} (-1)^{T_{\mathcal{P}}} g_{\nu_1 \mathcal{P}(a_1)} \dots g_{\nu_n \mathcal{P}(a_n)}, \quad (66)$$

where $T_{\mathcal{P}}$ is the number of inversions in the permutation \mathcal{P} of the n numbers a_1, \dots, a_n .

By applying the general definition 65, we find that in 4 dimensions we have

$$E_4 \equiv G = R^{\alpha\beta\gamma\delta} R_{\alpha\beta\gamma\delta} - 4 R^{\alpha\beta} R_{\alpha\beta} + R^2,$$

A.3 Vanishing of the Euler counterterms

In this section, we outline the proof of the claim made at the end of section 4, that the Euler counterterm vanishes in $d = 4$, as all the derivatives of the integrated Euler density, which is a topological invariant. Explicit calculations can be found in the notebook *vanishing_euler_ct.nb*. The derivation is inspired by the discussion of the three point function in Appendix A.2 of [4].

In order to do so, we exploit the fact that in d dimensions only d momenta can be independent. If we have d such momenta available, then the metric is not an independent tensor and we can rewrite it as

$$\delta^{\mu\nu} = \sum_{j,k=1}^d p_j^\mu p_k^\nu \left(Z^{-1} \right)_{kj}, \quad (67)$$

where Z is the Gram matrix, i.e. $Z_{ij} = (p_i \cdot p_j)_{k,j=1}^d$. Since, except for specific kinematic configurations, a general n -point function depends on $n - 1$ independent momenta, because of momentum conservation, if $n = d$, we can construct the n -th independent momentum using the completely antisymmetric Levi-Civita tensor,

$$n^\mu = \epsilon^{\mu\mu_2 \dots \mu_n} p_2 \dots p_n. \quad (68)$$

By construction n^μ is orthogonal to all of the other $n - 1$ momenta. In our case we have $n = d = 4$, so we can define our vector n^μ in terms of p_2, p_3 and p_4 .

Our Gram matrix is given by

$$\begin{pmatrix} p_2^2 & p_2 \cdot p_3 & p_2 \cdot p_4 & 0 \\ p_3 \cdot p_2 & p_3^2 & p_3 \cdot p_4 & 0 \\ p_4 \cdot p_2 & p_4 \cdot p_3 & p_4^2 & 0 \\ 0 & 0 & 0 & n^2 \end{pmatrix}, \quad (69)$$

with $n^2 = (p_2 \cdot p_3)^2 p_4^2 + (p_2 \cdot p_4)^2 p_3^2 + (p_3 \cdot p_4)^2 p_2^2 - 2 (p_2 \cdot p_3) (p_2 \cdot p_4) (p_3 \cdot p_4) - p_2^2 p_3^2 p_4^2$.

If we compute the inverse Gram matrix and apply (67) to $D_G^{\mu_1 \nu_1 \mu_2 \nu_2 \mu_3 \nu_3 \mu_4 \nu_4}(p_1, p_2, p_3, p_4)$, we can check that, indeed, the Euler counterterm vanishes.

In our notebook, we first check that all of the traces of the re-expressed Euler counterterm are zero, if up to two indices pair are left open, i.e.

$$\begin{aligned} \delta_{\mu_1 \nu_1}^{(4)} \delta_{\mu_2 \nu_2}^{(4)} \delta_{\mu_3 \nu_3}^{(4)} \delta_{\mu_4 \nu_4}^{(4)} D_G^{\mu_1 \nu_1 \mu_2 \nu_2 \mu_3 \nu_3 \mu_4 \nu_4}(p_1, p_2, p_3, p_4) &= 0, \\ \delta_{\mu_2 \nu_2}^{(4)} \delta_{\mu_3 \nu_3}^{(4)} \delta_{\mu_4 \nu_4}^{(4)} D_G^{\mu_1 \nu_1 \mu_2 \nu_2 \mu_3 \nu_3 \mu_4 \nu_4}(p_1, p_2, p_3, p_4) &= 0, \\ \delta_{\mu_3 \nu_3}^{(4)} \delta_{\mu_4 \nu_4}^{(4)} D_G^{\mu_1 \nu_1 \mu_2 \nu_2 \mu_3 \nu_3 \mu_4 \nu_4}(p_1, p_2, p_3, p_4) &= 0. \end{aligned} \quad (70)$$

These preliminary tests are not very informative, in fact, for if we consider the trace Ward identities for the Euler counterterm in d dimensions, we see from (49) to (51) that the traces with four, three and two traced indices pairs must vanish also for $d \neq 4$. On the other hand, if we have only one traced pair, we see that the rhs of (51) in $d = 4$ is given by a symmetric combination of the 3-point Euler counterterms. Thus, proving that

$$\delta_{\mu_1 \nu_1}^{(4)} D_G^{\mu_1 \nu_1 \mu_2 \nu_2 \mu_3 \nu_3 \mu_4 \nu_4}(p_1, p_2, p_3, p_4) = 0. \quad (71)$$

actually holds is the first non trivial test one can make. One can observe that since the symmetric combination in the rhs of (51) certainly does not vanish in $d \neq 4$, then (71) is a non trivial check of the fact that also the 3-point function counterterm must vanish for $d = 4$. Indeed, its explicit form involves the projector onto the space of fully antisymmetric 5-indices tensors [1], which is necessarily zero for integer $d < 5$. This is also explicitly shown in our code.

Finally, we perform the same check for the fully uncontracted Euler counterterm, actually finding out that

$$D_G^{\mu_1 \nu_1 \mu_2 \nu_2 \mu_3 \nu_3 \mu_4 \nu_4}(p_1, p_2, p_3, p_4) = 0. \quad (72)$$

The full tests with all the necessary comments and details can be found in our repository.

B Functional derivatives

B.1 Basic functional derivatives

Here we give the basic momentum space functional derivatives, which are the building blocks needed to for all of the counterterms, vertices and anomalies. Once these few formulas are understood, the construction of all the rest is a matter of (very) careful bookkeeping and a lot of applications of the chain rule for functional derivatives: please notice that in the following formulas terms which vanish in the flat space-time limit are already dropped, but one must take them into account for higher order derivatives.

$$[g_{\alpha\beta}]^{\mu_1 \nu_1}$$

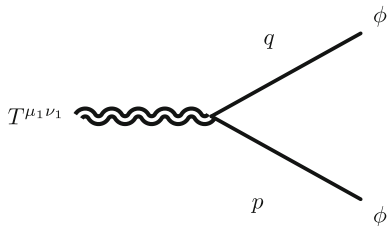
$$\begin{aligned}
 &= \frac{1}{2} \left(\delta_\alpha^{\mu_1} \delta_\beta^{\nu_1} + \delta_\alpha^{\nu_1} \delta_\beta^{\mu_1} \right), \\
 &[g^{\alpha\beta}]^{\mu_1\nu_1} \\
 &= -\frac{1}{2} \left(\delta^{\mu_1\alpha} \delta^{\nu_1\beta} + \delta^{\nu_1\alpha} \delta^{\mu_1\beta} \right), \\
 &[\sqrt{g}]^{\mu_1\nu_1} \\
 &= \frac{1}{2} g^{\mu_1\nu_1}, \\
 &[\Gamma_{\beta\chi}^\alpha]^{\mu\nu}(k) \\
 &= \frac{i}{2} \delta^{\alpha\lambda} \left(-[g_{\beta\chi}]^{\mu\nu} k_\lambda + [g_{\beta\lambda}]^{\mu\nu} k_\chi + [g_{\lambda\chi}]^{\mu\nu} k_\beta \right), \\
 &[\Gamma_{\alpha\beta\chi}]^{\mu\nu}(k) \\
 &\equiv \delta_{\alpha\delta} [\Gamma_{\beta\chi}^\delta]^{\mu\nu}(k) \\
 &[\Gamma_{\beta\chi}^\alpha]^{\mu_1\nu_1\mu_2\nu_2}(k_1, k_2) \\
 &= [g^{\alpha\lambda}]^{\mu_1\nu_1} [\Gamma_{\lambda\beta\chi}]^{\mu_2\nu_2}(k_2) + (1 \rightarrow 2), \\
 &[\Gamma_{\beta\chi}^\alpha]^{\mu_1\nu_1\mu_2\nu_2\mu_3\nu_3}(k_1, k_2, k_3) \\
 &= [g^{\alpha\lambda}]^{\mu_1\nu_1\mu_2\nu_2} [\Gamma_{\lambda\beta\chi}]^{\mu_3\nu_3}(k_3) + (1 \leftrightarrow 2, 1 \rightarrow 3).
 \end{aligned}
 \tag{73}$$

All further details are given in the file *all_functional_derivatives_computed.nb*

B.2 Interaction vertices of the scalar field with gravitons

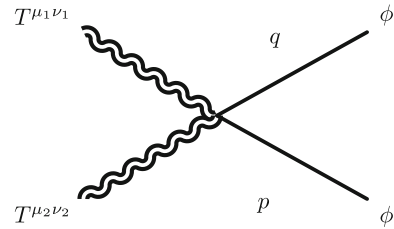
We provide here the explicit forms of the three vertices used in the Feynman diagrams. The computation of the vertices can be done by taking at most three functional derivatives of the scalar action in curved space with respect to the metric tensor and, of course, the scalar field. This is because the vev's of the fourth order derivatives correspond to massless tadpoles, which are set to zero in DR, so no fourth derivative is needed.

- graviton - scalar - scalar vertex



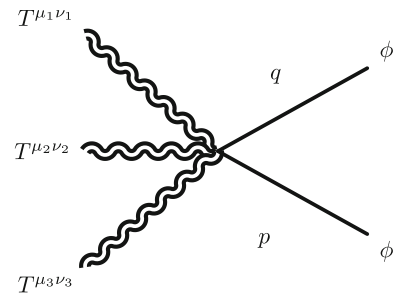
$$\begin{aligned}
 V_{H\phi\phi}^{\mu\nu}(\mathbf{p}, \mathbf{q}) &= \frac{1}{2} \left(\delta^{\mu\alpha} \delta^{\nu\beta} - \frac{1}{2} \delta^{\mu\nu} \delta^{\alpha\beta} \right) (p_\alpha q_\beta + p_\beta q_\alpha), \\
 &+ \chi \left(\delta^{\mu\nu} \delta^{\alpha\beta} - \delta^{\mu\alpha} \delta^{\nu\beta} \right) \\
 &\left(p_\alpha p_\beta + p_\alpha q_\beta + q_\alpha p_\beta + q_\alpha q_\beta \right),
 \end{aligned}$$

- graviton - graviton - scalar - scalar vertex



$$\begin{aligned}
 V_{HH\phi\phi}^{\mu\nu\rho\sigma}(\mathbf{p}, \mathbf{q}, \mathbf{l}) &= \frac{1}{2} \left([\sqrt{g}]^{\rho\sigma} \left(\delta^{\mu\alpha} \delta^{\nu\beta} - \frac{1}{2} \delta^{\mu\nu} \delta^{\alpha\beta} \right) \right. \\
 &+ \left. \left[g^{\mu\alpha} g^{\nu\beta} - \frac{1}{2} g^{\mu\nu} g^{\alpha\beta} \right]^{\rho\sigma} \right) (p_\alpha q_\beta + p_\beta q_\alpha), \\
 &+ \chi \left\{ \left[[\sqrt{g}]^{\rho\sigma} \left(\delta^{\mu\nu} \delta^{\alpha\beta} - \delta^{\mu\alpha} \delta^{\nu\beta} \right) \right. \right. \\
 &+ \left. \left. \left[g^{\mu\nu} g^{\alpha\beta} - g^{\mu\alpha} g^{\nu\beta} \right]^{\rho\sigma} \right) \right. \\
 &\left. \left(p_\alpha p_\beta + p_\alpha q_\beta + p_\beta q_\alpha + q_\alpha q_\beta \right) \right. \\
 &+ \left. \left(\delta^{\mu\nu} \delta^{\alpha\beta} - \delta^{\mu\alpha} \delta^{\nu\beta} \right) \left[\Gamma_{\alpha\beta}^\lambda \right]^{\rho\sigma}(\mathbf{l}) i (p_\lambda + q_\lambda) \right. \\
 &\left. - \left(\frac{1}{2} \delta^{\mu\nu} \delta^{\alpha\beta} - \delta^{\mu\alpha} \delta^{\nu\beta} \right) \left[R_{\alpha\beta} \right]^{\rho\sigma}(\mathbf{l}) \right\},
 \end{aligned}$$

- graviton - graviton - scalar - scalar vertex



$$\begin{aligned}
 V_{HHH\phi\phi}^{\mu\nu\rho\sigma\chi\omega}(\mathbf{p}, \mathbf{q}, \mathbf{l}_1, \mathbf{l}_2) &= \frac{1}{2} \left\{ [\sqrt{g}]^{\rho\sigma\chi\omega} \right. \\
 &\times \left(\delta^{\mu\alpha} \delta^{\nu\beta} - \frac{1}{2} \delta^{\mu\nu} \delta^{\alpha\beta} \right) \\
 &+ [\sqrt{g}]^{\rho\sigma} \left[g^{\mu\alpha} g^{\nu\beta} - \frac{1}{2} g^{\mu\nu} g^{\alpha\beta} \right]^{\chi\omega} \\
 &+ [\sqrt{g}]^{\chi\omega} \left[g^{\mu\alpha} g^{\nu\beta} - \frac{1}{2} g^{\mu\nu} g^{\alpha\beta} \right]^{\rho\sigma} \\
 &+ \left. \left[g^{\mu\alpha} g^{\nu\beta} - \frac{1}{2} g^{\mu\nu} g^{\alpha\beta} \right]^{\rho\sigma\chi\omega} \right\} (p_\alpha q_\beta + p_\beta q_\alpha) \\
 &+ \chi \left\{ [\sqrt{g}]^{\rho\sigma\chi\omega} \left(\delta^{\mu\nu} \delta^{\alpha\beta} - \delta^{\mu\alpha} \delta^{\nu\beta} \right) \right. \\
 &+ [\sqrt{g}]^{\rho\sigma} \left[g^{\mu\nu} g^{\alpha\beta} - g^{\mu\alpha} g^{\nu\beta} \right]^{\chi\omega} \\
 &+ [\sqrt{g}]^{\chi\omega} \left[g^{\mu\nu} g^{\alpha\beta} - g^{\mu\alpha} g^{\nu\beta} \right]^{\rho\sigma} \\
 &+ \left. \left[g^{\mu\nu} g^{\alpha\beta} - g^{\mu\alpha} g^{\nu\beta} \right]^{\rho\sigma\chi\omega} \right\} \\
 &\times (p_\alpha p_\beta + p_\alpha q_\beta + q_\alpha p_\beta + q_\alpha q_\beta)
 \end{aligned}$$

$$\begin{aligned}
& + \chi \left\{ \left([\sqrt{g}]^{\chi\omega} [\delta^{\mu\nu} \delta^{\alpha\beta} - \delta^{\mu\alpha} \delta^{\nu\beta}] \right. \right. \\
& + \left. \left. [g^{\mu\nu} g^{\alpha\beta} - g^{\mu\alpha} g^{\nu\beta}]^{\chi\omega} \right) [\Gamma_{\alpha\beta}^{\lambda}]^{\rho\sigma} (\mathbf{l}_1) \right. \\
& + (\rho, \sigma, l_1) \leftrightarrow (\tau, \omega, l_2) \\
& + \left. \left. (\delta^{\mu\nu} \delta^{\alpha\beta} - \delta^{\mu\alpha} \delta^{\nu\beta}) [\Gamma_{\alpha\beta}^{\lambda}]^{\rho\sigma\chi\omega} (\mathbf{l}_1, \mathbf{l}_2) \right\} i (p_\lambda + q_\lambda) \\
& + \chi \left\{ \left([\sqrt{g}]^{\chi\omega} \left(\delta^{\mu\alpha} \delta^{\nu\beta} - \frac{1}{2} \delta^{\mu\nu} \delta^{\alpha\beta} \right) \right. \right. \\
& + \left. \left. [g^{\mu\alpha} g^{\nu\beta} - \frac{1}{2} g^{\mu\nu} g^{\alpha\beta}]^{\chi\omega} \right) [R_{\alpha\beta}]^{\rho\sigma} (\mathbf{l}_1) \right. \\
& + (\rho, \sigma, l_1) \leftrightarrow (\tau, \omega, l_2) \\
& + \left. \left. \left(\delta^{\mu\alpha} \delta^{\nu\beta} - \frac{1}{2} \delta^{\mu\nu} \delta^{\alpha\beta} \right) [R_{\alpha\beta}]^{\rho\sigma\chi\omega} (\mathbf{l}_1, \mathbf{l}_2) \right\}
\end{aligned}$$

References

1. H. Osborn, A.C. Petkou, Implications of conformal invariance in field theories for general dimensions. *Ann. Phys.* **231**, 311 (1994). [arXiv:hep-th/9307010](#)
2. J. Erdmenger, H. Osborn, Conserved currents and the energy momentum tensor in conformally invariant theories for general dimensions. *Nucl. Phys. B* **483**, 431 (1997). [arXiv:hep-th/9605009](#)
3. C. Corianò, L. Delle Rose, E. Mottola, M. Serino, Solving the conformal constraints for scalar operators in momentum space and the evaluation of Feynman's master integrals. *JHEP* **07**, 011 (2013). [arXiv:1304.6944](#)
4. A. Bzowski, P. McFadden, K. Skenderis, Implications of conformal invariance in momentum space. *JHEP* **03**, 111 (2014). [arXiv:1304.7760](#)
5. A. Bzowski, P. McFadden, K. Skenderis, Renormalised 3-point functions of stress tensors and conserved currents in CFT. *JHEP* **11**, 153 (2018). [arXiv:1711.09105](#)
6. C. Corianò, E. Delle Rose, E. Mottola, M. Serino, Graviton vertices and the mapping of anomalous correlators to momentum space for a general conformal field theory. *JHEP* **1208**, 147 (2012). [arXiv:1203.1339](#)
7. C. Corianò, M.M. Maglio, The general 3-graviton vertex (TTT) of conformal field theories in momentum space in $d = 4$. *Nucl. Phys. B* **937**, 56 (2018). [arXiv:1808.10221](#)
8. A.M. Polyakov, Conformal symmetry of critical fluctuations. *JETP Lett.* **12**, 381 (1970)
9. M.S. Costa, J. Penedones, D. Poland, S. Rychkov, Spinning conformal correlators. *JHEP* **11**, 071 (2011). [arXiv:1107.3554](#)
10. S. Ferrara, A. Grillo, R. Gatto, Tensor representations of conformal algebra and conformally covariant operator product expansion. *Ann. Phys.* **76**, 161 (1973)
11. A. Polyakov, Nonhamiltonian approach to conformal quantum field theory. *Zh. Eksp. Teor. Fiz.* **66**, 23 (1974)
12. Simmons-Duffin, D.: the conformal bootstrap. In: Proceedings, theoretical advanced study institute in elementary particle physics: new frontiers in fields and strings (TASI 2015): Boulder, CO, USA, pp 1–74 (2017). [arXiv:1602.07982](#)
13. J.-F. Fortin, W. Skiba, Conformal bootstrap in embedding space. *Phys. Rev. D* **93**, 105047 (2016). [arXiv:1602.05794](#)
14. Fortin, J.-F., Skiba, W.: A recipe for conformal blocks (2019). [ArXiv:1905.00036](#)
15. J.-F. Fortin, V. Prilepina and W. Skiba, Conformal two-point correlation functions from the operator product expansion. [arXiv:1906.12349](#)
16. J.-F. Fortin, V. Prilepina and W. Skiba, Conformal three-point correlation functions from the operator product expansion (2019). [arXiv:1907.08599](#)
17. J.-F. Fortin, V. Prilepina, W. Skiba, Conformal four-point correlation functions from the operator product expansion (2019). [arXiv:1907.10506](#)
18. A. Dymarsky, On the four-point function of the stress-energy tensors in a CFT. *JHEP* **10**, 075 (2015). [arXiv:1311.4546](#)
19. G. Chalmers, J. Erdmenger, Dual expansions of N=4 superYang-Mills theory via IIB superstring theory. *Nucl. Phys. B* **585**, 517 (2000). [arXiv:hep-th/0005192](#)
20. V. Didenko, E. Skvortsov, Exact higher-spin symmetry in CFT: all correlators in unbroken Vasiliev theory. *JHEP* **04**, 158 (2013). [arXiv:1210.7963](#)
21. V. Didenko, J. Mei, E. Skvortsov, Exact higher-spin symmetry in CFT: free fermion correlators from Vasiliev Theory. *Phys. Rev. D* **88**, 046011 (2013). [arXiv:1301.4166](#)
22. C. Sleight, M. Taronna, Higher spin interactions from conformal field theory: the complete cubic couplings. *Phys. Rev. Lett.* **116**, 181602 (2016). [arXiv:1603.00022](#)
23. R. Bonezzi, N. Boulanger, D. De Filippi, P. Sundell, Noncommutative Wilson lines in higher-spin theory and correlation functions of conserved currents for free conformal fields. *J. Phys. A* **50**, 475401 (2017). [arXiv:1705.03928](#)
24. G.P. Korchemsky, E. Sokatchev, Four-point correlation function of stress-energy tensors in $\mathcal{N} = 4$ superconformal theories. *JHEP* **12**, 133 (2015). [arXiv:1504.07904](#)
25. H.H. Patel, Package-X: a mathematica package for the analytic calculation of one-loop integrals. *Comput. Phys. Commun.* **197**, 276 (2015). [arXiv:1503.01469](#)
26. H.H. Patel, Package-X 2.0: a mathematica package for the analytic calculation of one-loop integrals. *Comput. Phys. Commun.* **218**, 66 (2017). [arXiv:1612.00009](#)
27. A. Denner, S. Dittmaier, Reduction of one loop tensor five point integrals. *Nucl. Phys. B* **658**, 175 (2003). [arXiv:hep-ph/0212259](#)
28. A. Denner, S. Dittmaier, Reduction schemes for one-loop tensor integrals. *Nucl. Phys. B* **734**, 62 (2006). [arXiv:hep-ph/0509141](#)
29. A. Denner, S. Dittmaier, Scalar one-loop 4-point integrals. *Nucl. Phys. B* **844**, 199 (2011). [arXiv:1005.2076](#)
30. A. Denner, S. Dittmaier, L. Hofer, Collier: a fortran-based complex one-loop library in extended regularizations. *Comput. Phys. Commun.* **212**, 220 (2017). [arXiv:1604.06792](#)
31. M. Serino, Conformal anomaly actions and Dilaton interactions (INFN, Lecce, 2014). [arXiv:1407.7113](#)
32. A. Iorio, L. O'Raifeartaigh, I. Sachs, C. Wiesendanger, Weyl gauging and conformal invariance. *Nucl. Phys. B* **495**, 433 (1997). [arXiv:hep-th/9607110](#)
33. M.J. Duff, Observations on conformal anomalies. *Nucl. Phys. B* **125**, 334 (1977)
34. N.D. Birrell, P.C.W. Davies, *Quantum Fields in Curved Space*, Cambridge Monographs on Mathematical Physics. (Cambridge University Press, Cambridge, 1984). <https://doi.org/10.1017/CBO9780511622632>.
35. L. Bonora, P. Cotta-Ramusino, C. Reina, Conformal anomaly and cohomology. *Phys. Lett. B* **126**, 305 (1983)
36. I. Antoniadis, P.O. Mazur, E. Mottola, Conformal symmetry and central charges in four-dimensions. *Nucl. Phys. B* **388**, 627 (1992). [arXiv:hep-th/9205015](#)
37. C. Corianò, L. Delle Rose, M. Serino, Three and four point functions of stress energy tensors in D=3 for the analysis of cosmological non-gaussianities. *JHEP* **1212**, 090 (2012). [arXiv:1210.0136](#)
38. T. Ohl, Drawing Feynman diagrams with LaTeX and Metafont. *Comput. Phys. Commun.* **90**, 340 (1995). [arXiv:hep-ph/9505351](#)
39. D. Capper, M. Duff, Trace anomalies in dimensional regularization. *Nuovo Cim. A* **23**, 173 (1974)

40. G. Passarino, M. Veltman, One loop corrections for $e^+ e^-$ annihilation into $\mu^+ \mu^-$ in the Weinberg model. Nucl. Phys. B **160**, 151 (1979)
41. C. Corianò, L. Delle-Rose, C. Marzo, M. Serino, Higher order Dilaton interactions in the nearly conformal limit of the standard model. Phys. Lett. B **717**, 182 (2012). [arXiv:1207.2930](https://arxiv.org/abs/1207.2930)
42. C. Corianò, L. Delle Rose, C. Marzo, M. Serino, Conformal trace relations from the Dilaton Wess-Zumino action (2013). [arXiv:1306.4248](https://arxiv.org/abs/1306.4248)
43. S. Deser, A. Schwimmer, Geometric classification of conformal anomalies in arbitrary dimensions. Phys. Lett. B **309**, 279 (1993). [arXiv:hep-th/9302047](https://arxiv.org/abs/hep-th/9302047)